**UNIVERSITY OF PISA**

**Research Doctorate School in**
**BIOLOGICAL AND MOLECULAR SCIENCES**

**Course in**
**EXPERIMENTAL AND MOLECULAR ONCOLOGY**

**XXIII CYCLE (2008-2010)**

***Research Doctorate Thesis***

# Molecular targeting and development of a new radioreceptor therapeutic strategy for non-iodophil epithelial follicular thyroid and neuroendocrine-like tumors.

***Supervisor***

**Prof. Giuliano Mariani**

***Tutor***

**Dr. Paola Anna Erba**

***Candidate***

**Dr. Chiara Manfredi**

*“I have no particular talent.*
*I am passionately curious”.*

*Albert Einstein*

*“Somewhere, something*
*incredible is waiting to be known”.*

*Carl Sagan*

*To all those that I have been*
*passionate about science.*

# TABLE OF CONTENTS

# ABBREVIATIONS

| | |
|---|---|
| ACTH | Adrenocorticotropic Hormone |
| CCL39 | Chinese Hamster lung fibroblast cell line |
| CHO | Chinese Hamster Ovary cancer cell line |
| CNS | Central nervous system |
| DCM | Dichloromethane |
| DMF | Dimethylformamide |
| DOTA | 1,4,7,10-tetraazacyclododecane-1,4,7,10-tetraacetic acid |
| DTPA | Diethylentriaminepentaacetic acid |
| EGF | Epidermal growth factor |
| GEP | Gastroentropancreatic |
| GF | Growth factor |
| GH | Growth hormone |
| GPCR | G-protein coupled receptor |
| HEK | Human embryonic kidney (cells) |
| hSSTR | Human somatostatin receptor |
| HYNIC | 2-hydrazinonicotinic acid |
| IFN-γ | Interferon- γ |
| IGF-1 | Insuline-like growth factor |
| IL-1 | Interleukine-1 |
| MEN | Multiple endocrine neoplasia |
| mRNA | Messenger ribonucleic acid |
| MTC | Medullary thyroid cancer |
| NET | Neuroendocrine tumor |
| nNOS | Neuronal Nitric Oxide Synthase |
| p.i. | Post injection |
| PTP | Phoshotyrosine phosphatases |
| RCCC | Renal clear cell carcinoma |
| RT-PCR | Reverse Trascrittase Polymerase chain reaction |
| PDGF | Platelet-derived growth factor |
| PET | Positron emission tomography |
| PRRT | Peptide receptor radionuclide therapy |
| RP-HPLC | Reverse phase-high performance liquid cromatography |
| SPECT | Single photon emission computer tomography |
| SRIF | Somatotropin release-inhibiting factor |
| SHP-1 | SH2 domain-containing phosphatases |
| SST | Somatostatin |
| SSTR | Somatostatin receptor |
| TSH | Thyroid-stimulating hormone |
| TUNEL | Terminal deoxynucleotidyl transferase dUTP nick end labeling |
| VEGF | Vascular endothelial growth factor |

# INTRODUCTION

## 1. Somatostatin and its receptor family.

### 1.1 Somatostatin and it actions.

Somatostatin (somatotropin release-inhibiting factor, SRIF or SST) was identified in the hypothalamus as a tetradecapeptide with the goal of inhibiting the release of growth hormone (GH)[1]. Subsequently it was discovered that the human SST gene encodes a precursor prohormone, that is enzimatically cleaved to yield the two bioactive forms of SST: the first is composed by 14 aminoacids (SST-14), while the second by 28 aminoacids (SST-18). Both SST-14 and SST-28 are found in circulation, secreted not only from hypothalamus but, from gastrointestinal tract, the central and peripheral nervous system and to a lesser extent, other endocrine glands and reproductive organs[2]. SST functions as a neurotransmitter in the central nervous system (CNS) and as a regulator of endocrine and gastrointestinal functions[1,3]. SST inhibits hormone release, in particular GH, TSH, insulin and gut hormones, affects gastrointestinal function (inhibits gut exocrine secretion, regulates intestinal absorption, and decreases mucosal proliferation) and serves as neurotransmitter or neuromodulator. SST also blocks the release of growth factors (IGF-1, EGF, PDGF) and cytokines (IL-6, IFN-γ)[4,5,6].

These actions are mediated by a family of seven transmembrane domain G-protein coupled receptors composed by five different subtypes of SSTR. These are termed Somatostatin receptors 1-5 (SSTR1–SSTR5) and are encoded on five different chromosome[7,8]. These receptor subtypes all share common signal pathways of signal transduction involving adenylate cyclase, $Ca^{2+}$-$K^{+}$ channels and $Na^{+}/H^{+}$ exchanger and protein dephosphorylation[8] and bring to inhibitory effects on cellular processes such as secretion and cell proliferation[7].

## 1.2 Somatostatin receptors and their expression in normal tissues.

SSTR1-5 are five different receptors belonging to the same family, encoded by five different genes located on separate chromosomes. SSTR2 can be found in two different isoforms: SSTR2a or SSTR2b, obtained by two forms of alternative splicing, that led to a long variant (SSTR2a) or a short one (SSTR2b). The two isoforms differs only in the length of the cytoplasmic tail. The two variants are present in human too.

Thus, there are six putative SSTRs subtypes composed by 356-391 aminoacid residues. Each receptor is composed by seven α-helix trans-membrane domains typical of G-protein coupled receptors. The individual subtypes display a remarkable degree of structural conservation across species. SSTR1 presents 94-98% sequence identity between human, rat and mouse isoforms; SSTR2 presents 93-96% sequence identity between human rat, mouse, porcine and bovine isoforms. SSTR4 presents 88% of sequence identity between the rat and the human isoforms. SSTR3 and SSTR5 are less conserved and show an homology of 82%-83% between human and rodent isoforms.

The transmembrane domains have a great similarity in sequence, while the carboxy- and amino-terminal sequences are different from each other[20].
Somatostatin receptors were identify in different tissue using different technologies such as receptor binding studies, RT-PCR and immunohistochemistry and it was determined that SSTRs are expressed throughout the body including the CNS[9], particularly in brain and in peripheral organs including GI tract[10,11], endocrine and exocrine pancreas[12,13,14], kidney[15], pituitary, thyroid, adrenals and immune cells[16,17,18,19,20,21]. SSTR2a is the most expressed SST receptor and particularly, there is a very high expression in pancreatic islet and in peripheral nervous system, but also in adrenals, immune system and in kidney. SSTR4 is expressed in foetal and adult lungs, while a good expression of SSTR3-5 was demonstrated in T-lymphocytes.

## 1.3 Somatostatin receptor subtypes expression in human cancers.

Several studies demonstrated that different tumours express or overexpress a particular or several membrane receptor subtypes on their cellular membrane compared to the correspondent healthy organs[22]. SSTRs were the first receptor family to be identify in tumors. In particular, it is now well described and documented their expression in some malignancies[22,23]. The majority of human SSTR-positive tumors simultaneously express multiple SSTR subtypes, although there is a considerable variation in SST subtype expression between the different tumor types and among tumors of the same type. The presence of SSTRs in cancers was demonstrated by molecular biology with mRNA level using *in situ* hybridazation[24,25], RNase protection assays methodologies and RT-PCR[26,33], or by immunohistochemistry

adopting specific antibody against synthetic peptide sequences of the SSTR1-5[27]. It is by the combination of these different technique that more accurate results are obtained. SSTR2 is the most expressed receptor subtype in the majority of tumors[28].

There are some malignancies that express SSTRs. The most common SSTRs expressing tumors are: neuroendocrine tumors (NET)[29] and gastroenteropancreatic tumors (GEP)[30,31]. Characteristic of these cancer types is the interface between the endocrine (hormonal) system and the nervous system. NETs derive from diffused neuroendocrine system and, this is the consequence because, NETs can spread to different parts of the body. NETs are a heterogeneous group of neoplasm, originating from neural crest, that can be classified in two different sub-groups: the first and most common, is composed by well-differentiated and slowly-growing tumors, the second composed by rare pathologies, is made by poorly differentiated and malignant tumors with an aggressive behaviour. NET tumors includes: pituitary tumors[32,33], pheochromocytoma[34], meningioma[35], glioma[36], head and neck tumours[37], paragangliomas[38], medullary thyroid carcinomas (MTCs)[39], small cell lung cancer[40].

Endocrine tumors of the gastroenteropancreatic (GEP) axis (involving the gastrointestinal system, stomach, and pancreas) are rare, generally slow-growing tumors that occur in the pancreas and the gastrointestinal tract, which includes the stomach, small and large intestine[41].

They have a common embryologic origin, indicated by the term "protodifferentiated stem cell," and it is now believed to derive from the endoderm and capable of giving rise to a variety of tumors.

GEP tumors include carcinoid tumors and pancreatic endocrine tumors (also called pancreatic islet cell tumors). GEP tumors includes: carcinoid tumors, islet cells carcinomas[42] of the pancreas such as gastrinomas, glucoganomas,

GRFomas, vipomas, insulinomas, non functioning islet cells carcinomas, midgut and gastrointestinal tumors.

Moreover, there are two hereditary pathologies that have as consequent the establishment of different kinds of expressing SSTRs NET. These are: Multiple Endocrine Neoplasia, type 1 (MEN-1) and Multiple Endocrine Neoplasia type IIa-b (MEN-2a/b).

MEN-1 is a hereditary syndrome and is characterized by the presence of parathyroid glands, pancreatic islet cells, and pituitary gland[43,44,45] tumors. These tumor insurance is associated with the loss of a tumor suppressor gene on chromosome 11q13[46,47]. Moreover, it seems that allelic loss might be responsible for sporadic parathyroid and pituitary tumors as well as stomach, pancreas, and intestine[48,49,50] NETs.

The second is Multiple Endocrine Neoplasia type 2a (MEN-2a) syndrome is characterized by the occurrence of the following tumors: pheochromocytomas, medullary thyroid carcinomas (MTC) and parathyroid hyperplasia.

Multiple endocrine neoplasia type IIb (MEN-2b), has stigmata of cutaneous and mucosal neuromas and is not associated with parathyroid hyperplasia. MEN-2a, MEN-2b and familial MTCs are associated with RET protooncogene[51,52] mutations, a conventional dominant oncogene located on 10q11.2 chromosome. Although mutations in this region have been associated with sporadic MTC, the role of this gene in sporadic GEP tumors is not known.

Finally, the presence of SSTRs have been demonstrated both *in vitro* and *in vivo* in some other not endocrines malignancies such as adenocarcinomas of the breast[53], kidney[53,53], prostate[54], de-differentiated papillary and follicular thyroid cancer[55], ovary, lymphomas[56].

De-differetiated thyroid cancer includes papillary thyroid cancer (PTC). This pathology is usually curable by the combination of surgery, radioiodine ablation, and thyroid-stimulating hormone suppressive therapy, but recurrence occurs in 20–40% of patients[57]. During tumor progression, cellular dedifferentiation occurs in up to 5% of cases and it is usually accompanied by more aggressive growth, metastatic spread, and loss of iodide uptake ability, making the tumor resistant to the traditional therapeutic modalities and radioiodine. Along with the loss of radioiodine concentrating ability, de-differentiated thyroid cells develop some features typical of other tumors such as NETs. Beside the occurrence of transition from follicular epithelial thyroid cancer to medullary thyroid cancer, the expression of SSTRs on thyroid cells has recently been documented, demonstrating that these tumors highly express SSTR-1, SSTR-3, SSTR-5[58].

In conclusion, from the current scientific literature, it can be asserted that:

- SSTR2 is the most frequently expressed SSTR subtype in a majority of cancers;
- There is a high heterogeneity in the expression of individual SSTR within and between different tumors;
- SSTR1-2-3-5 are often found in GEP tumors, MTCs and in ephitelial ovarian cancers;
- SSTR3 is overexpressed in thymomas and inactive pituitary adenomas;
- Human cervical and endometrial cancers has a great expression of SSTR1-2-3;
- SSTR2-3-5 were found in human lung cancers;
- GH-secreting pituitary adenomas express SSTR2-5;

- non-iodophil follicular epithelial thyroid cancer expresses SSTR-1, SSTR-3, SSTR-5.

The predominant expression of SSTR2 in so different kinds of tumor threw the basis of the successful clinical application of radiolabelled or not SST analogs (octapeptide) [see section 2.3].

## 1.4 Incidence and mortality.

NET has a low incidence on population (about 5 cases on 100,000 inhabitants that is 0.5% of the total of malignancies) but, in the last 30 years, incidence is growing up of about five times, while survival is the same.
Both men and women can be affected by NETs, but an higher frequency is recorded in middle age (40-45 years old) and old (70-75 years old) male[59]. Children are attacked too.
In Italy, every year 1,200 new NET diagnosis are registered. Diagnosis is often difficult, because typical symptoms are low and sometimes difficult to understand. These include: diffuse rash, abdominal cramps accompanied by diarrhoea.
GEP tumors are the most frequent type of SSTRs expressing tumors, corresponding to the 70% of the totality, while brunchopulmonary carcinoids represent more than 25%. Regarding entero-pancreatic district, enteron carcinoids represent 29% of the patients, while ductal and gastric carcinoids are less common. Finally, appendicular and pancreatic carcinoids[60] are quite rare.

## 1.5 Neuroendocrine tumors aetiology.

NETs aetiology still remains unknown. Carcinoids incidence is mainly considered sporadic.
Hereditary proneness is observed in MEN-1 syndromes. Hemminki[59] reports that less than 1% of Swedish has a carcinoid history in their family.
However, it seems that some ethnic groups are mainly predisposeded to be affected by neuroendocrine tumors. This suggests that hormonal and ethnic factors have an influx on the neuroendocrine tumors growth.

## 1.6 Gastroenteropancreatic tumors aetiology.

Around 80% of GEP NETs express somatostatin receptors (SSTRs) on their cellular membrane. Tumours expressing SSTRs often contain one or more receptor subtypes. In addition, recent studies have shown that such receptors are preferably expressed in well-differentiated forms, that some advanced tumours can loose a particular receptor subtype while keeping others[61].

***Stomach***

Stomach NETs correspond to 5% of all GEP tumors[62], but a more accurate data were obtained after endoscopy technique using.
The most diffused stomach NETs are carcinoids that can be divided into three groups, where prognosis represents the main difference between these groups.
These are:

- **type 1**, where the pathology is associated with chronic atrophic gastritis: it constitutes 70-80% of gastric carcinoids. Old women

(60-80 years) are prevalently attacked. It is a benign tumor. Only in rare cases show metastasis;

- **type 2,** it is associated with MEN-1: men and women are attacked with the same incidence;
- **type 3,** it is a sporadic tumor: it has a predilection for male. 70% of the cases are associated with metastasis and a strong therapeutic approach is required. It has a poor prognosis.

**Appendix.**

Appendix is a frequent site for carcinoids insurgence, but Modlin[62] demonstrated a progressive decrease of appendicular NETs in last years. Appendicular carcinoids rapresent 60-70% of all appendicular tumors, but only 0.3-0.5% of all the appendicectomy[63].

Only in rare cases, appenicular NETs symptoms are shown and a precise diagnosis come out with histological examinations after appendicectomy.

Appendicular tumor onset age is between the second/third life decade. Another incidence spike was observed between 70-74 years.

Appendicular carcinoids incidence is 2.1 higher in women compared to men[64].

Mayo Clinic case-report reported that only 4% of appendicular carcinoids has metastasis insurgence. This is the reason because survive rate is about 5 years in 95% of patients.

**Oesophaghagus.**

Primitive oesophaghagus NET are extremely rare (0.05% of all GEP tumors and less than 1% of the neoplasia of this organs)[60]. 60-70 year old men are

the most attacked.

Oesophaghagus tumors are divided in typical carcinoids, atypical carcinoids and neuroendocrine carcinoids with small or big cells[65]. The last one is very rare. Atypical carcinoids and small cells oesophaghagus NET have poor prognosis.

**Enteron**

Enteron NETs are more frequent. Black people, particularly male, are predominantly predisposed in this tumor growth.

Duodenum and proximal jejunum carcinoids are associated with Zollinger-Ellison syndrome, a pathology that demonstrated about 10 years of survival in 84% of the cases.

Other histotypes are: SST secreting tumors neurofibromatosis 1 associated or not, poorly differentiated carcinoids and ganglytic paragangliomas.

Distalis and ileal jejunum carcinoids are associated with carcinoid syndrome[66].

At diagnosis, about 60% of patients shows distant metastasis. Five years is the average of survival prognosis in 60% of patients.

**Colon and rectus.**

If colon NETs are extremely rare, rectus NETs represent about 20% of all GEP tumors[65]. In western counties, colon NETs are diagnosed during the seventh decade of life, while rectal carcinoids during the sixth[63].

Poorly differentiated colon tumors are typical and male are mostly attacked, while rectus tumors usually present differentiated tumoral cells. It is rare that colon and rectus syndromes could be associated to carcinoids.

**Pancreas.**

Pancreas NETs incidence is about 10/1.000.000 population/year. Women are mainly attacked, particularly during the third/fourth decade of life. Pancreas NET are 2% of all the pancreas neoplasia[67].

Pancreas NETs are divided into two groups: functional and not-functional, depending on whether a clinical syndrome resulting from the autonomously released hormone is present (gastrinoma, insulinoma, glaucagoma, VIPoma, somatostinoma, GRFHoma, ACTHoma). Not-functional tumors frequently release hormones and peptides (chromogranin A, pancreatic polypeptide, neurotensin, enolase) that do not cause distinct clinical syndromes. 90% of not-functional pancreatic NETs are malignant.

Not-functional pancreas NET corresponds to 15% of all pancreas tumors. Clinical showing is due to the tumoral mass effect on nearer organs. Cellular proliferation is usually slow but, at diagnosis, more than 50% of patients presents liver and lymph nodes metastatic diffusion.

Insulinomas are the most frequent functional pancreas NETs (about 70% of all pancreas NETs). 40-60 years old female shows an high insulinoma incidence. Diagnosis occurs early, because patients show an incorrect glucidic metabolism. 10% of insulinomas are included in MEN-1 panel.

20% of pancreas NETs are gastrinomas (incidence 4-10 case/1,000,000 persons/year). Maximal incidence are registered during the fourth decade of life. Symptoms are poor. 25-50% of the patients is affected by MEN-1.

VIPomas corresponds to 2-8% of pancreatic NETs, 70% of patients are women.

Glucoganomas represent 5% of all pancreatic NETs and 8% of all functional tumors. Even in this last case females are mostly attacked, incidence spike is obseved at 40 years.

Pancreatic cancers demonstrated an heterogeneous expression profile of SSTR subtype[68]. Somatostatin receptors have been extensively mapped in different pancreatic tumours by means of autoradiography, reverse-transcription polymerase chain reaction, in situ hybridization and immunohistochemistry; SSTR-1, -2, -3 and -5 are usually expressed in pancreatic NETs. Pancreatic insulinomas had heterogeneous SSTRs expression while 100% of somatostatinomas expressed SSTR 5 and 100% gastrinomas and glucagonomas expressed SSTR 2[69].

## 1.7 Medullary thyroid carcinoma.

Medullary thyroid carcinoma (MTC) arises from thyroid's parafollicular C cells. MTCs correspond to 5% of all thyroid cancers. It may occur as sporadic, as a component of the MEN-2b syndrome, or as familiar medullary thyroid cancer syndrome. These hereditary syndromes are autosomal dominant disorder and are caused by mutation of the *ret* proto-oncogene.
MTC patients typically present thyroid nodule, cervical adenopathy, distant disease, high level of circulating calcitonin and consequent flushing, pruritus and diarrhea. Other elements and typical features of MEN-2a/-2b are observed.

MTC demonstrated a coexpression of more than one SSTR. The presence of different SSTR subtypes mRNA were observed by RT-PCR with the exception of SSTR4 mRNA[70].

## 1.8 Follicular and Papillary Thyroid Cancer.

Thyroid cancer incidence increased 2.6-fold from 1973 to 2006. This change can be attributed primarily to an increase in papillary and follicular thyroid

carcinoma, which increased 3.2-fold ($P<0.0001$)[71]. Follicular and papillary thyroid cancers are generally characterised by excellent clinical outcome after conventional treatment (thyroidectomy and $^{131}I$ treatment). But during tumor progression, cellular dedifferentiation occurs in up to 5% of cases and is usually accompanied by more aggressive growth, metastatic spread, and loss of iodide uptake ability, making the tumor resistant to the traditional therapeutic modalities and radioiodine. Conventional chemotherapy and radiotherapy have a modest, if any, effect on advanced dedifferentiated thyroid cancer, which is responsible for a large number of deaths attributed to thyroid cancer. Various recent studies have described the visualization of metastases from follicular cell-derived thyroid carcinomas by means of somatostatin receptor scintigraphy although, in contrast to medullary thyroid carcinoma, these tumors are not of neuroendocrine origin. These findings are in agreement with the *in vitro* demonstration of specific somatostatin binding receptors in thyroid carcinoma cells. In the majority of these tumors, the expression of SSTR-1 seems to predominate, but a high positivity was observed in SSTR-3, and SSTR-5 expression too[72].

## 1.9 Lung.

Lung cancer is the most common cause of cancer death both in men and women throughout the word. The two main lung cancer type are: small cell lung cancer and non-small cell lung cancer and diagnosis occurs by microscopy. The American Cancer Society estimates that 219,440 new cases of lung cancer were diagnosed in the U.S. and 159,390 deaths due to lung cancer occur in 2009. In U.S., incidence on population is one out of every 14 men (almost 70% of people diagnosed with lung cancer are over 65 years of age, while less than 3% of lung cancers occur in people under 45 years of age). The management of pulmonary neuroendocrine tumours is poorly

standardised and data about somatostatin receptors (SSTR) expression or therapeutic guidelines for somatostatin analogue administration are still debated. From a study it was demonstrated that SSTR2a was strikingly overexpressed in metastatic typical carcinoids as compared with atypical carcinoids and clinically benign typical carcinoids[73].

## 1.10 Breast.

Breast cancer is the most common cancer disease among women[74]. Each year 210,000 new cases are diagnosed in U.S., of which 50,000 are ductal carcinoma *in situ* and 41,000 dies. Incidence continues to increase slowly, but mortality started to decrease from 1990s, thanks to mammographic screening, improvement of surgical techniques, radiation therapy and systemic adjuvant therapy, but about 1,000,000 new cases are diagnosed worldwide each year and death incidence dramatically changes in each nation. 5% of breast cancer are hereditary, however, the majority of breast cancers[75] are sporadic and are critically influenced by hormonal exposure to ovarian steroids[76]. Normal breast development, breast carcinogenesis as well as growth and progression of breast cancer depends on several hormones produced by the ovary (estrogens, progesteron), pituitary (GH, prolactin), and endocrine pancreas (insulin), as well as growth factors (epidermal growth factor, transforming growth factor, insulin-like growth factor) synthesized locally by normal or cancerous epithelial cells and by stromal cells. SSTR1-5 expression were determined in primary ductal breast tumors through semi-quantitative RT-PCR and immunocytochemistry. All five SSTR subtypes are variably expressed at the mRNA level in breast tumors

are localized to both tumor cells and the surrounding peritumoral regions as detected by immunocytochemistry[77].

## 1.11 Kidney.

Renal cell carcinoma (RCC) corresponds of about 2% of all cancer worldwide, and thanks to the increasing use of imaging techniques diagnosis occurs easily and it incidence is increasing till 1.5-5.5%[78]. RCC has a major lethality if compared to the other urinary tract tumors. Metastatic disease occurs in 30-40%[79] of RCC patients, and metastatic disease occurs 2 years after partial or total nephrectomy[80], while not treated metastatic RCC patients have a 5 years survival of 0-18%[81]. It was demonstrated by immunohistochemistry that not pathological kidney express SSTRs, SSTR-1 and 2a in glomus, while SSTR1-2-2a-2b-4-5 in tubule[16].

## 1.12 Lymphoma.

Lymphoma is a cancer in the lymphatic cells of the immune system and presents as a solid tumor of lymphoid cells. These malignant cells often originate in lymph nodes, presenting as an enlargement of the node. Lymphomas are closely related to lymphoid leukemias, which also originate in lymphocytes but typically involve only circulating blood and the bone marrow (where blood cells are generated in a process termed haematopoesis) and do not usually form static tumors. There are many types of lymphomas, and in turn, lymphomas are a part of the broad group of diseases called hematological neoplasms. Lymphomas represent 5.3% of all cancers in the United States and 55.6% of all blood cancers. Prognosis depends to the lymphoma type and stage. In particular, SSTRs are expressed in non-Hodgkin's lymphoma[82], lymphomas of the mucosa-associated lymphoid

tissue (MALT)-type arise in the stomach, but extragastric locations are also frequently encountered[83].

# 2 Somatostatin and it actions.

## 2.1 Somatostatin and it activation.

SST is encoded by a single gene and it mature form is obtained by two subsequent proteolitic cleavages that bring from the primitive pre-prosomatostatin to the prosomatostatin that is newly modified in the two final and mature products: 14 amino acids SST (SST-14) and 28 amino acids SST (SST-28)[28] (Figure 1). Pharmacological studies reveals that SST-14 and SST-28 binds to SSTR1-5 receptors with high affinity, but SST-28 has a 10 times higher affinity for SSTR-5 respect to SST-14.

SST functions were discovered in 1973 by Guillemin and Gerich[84]. It was isolated in the hypothalamus and researchers initially hypothesized that the only own function was to inhibit growth hormone release by pituitary gland. Subsequently, SST was discovered in most brain regions and in peripheral organs, but SST is typically contained in neurons or endocrine-like cells, such as central and peripheral nervous systems, in the endocrine pancreas and the gut, and in small number in the thyroid, adrenals, submandibular glands, kidney, prostate and placenta, where it executes different functions[7].

## 2.2 Somatostatin functions.

SST action is executed when it binds to it specific receptor. There are five SSTRs subtypes, composed by seven transmembrane domains and coupled by G-protein (Figure 2).

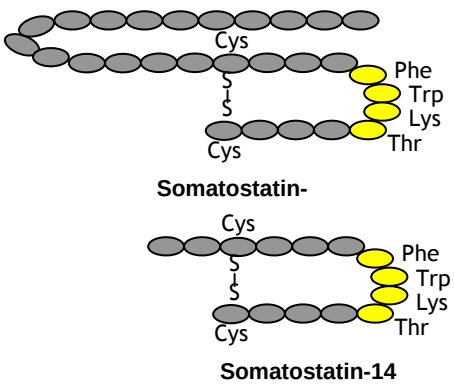


**Figure 1**: SST-28 and SST-14. The two forms have the same aminoacidic sequence, with the length is the only exceptions. The yellow dots represent the pharmacophore.

When the SST-SSTR binding occurs, the second messenger systems is activated. This system includes: inhibition of Adenylyl Cyclase, inhibition of calcium channels and activation of phospholipase-c. All these processes bring to the inhibition of the hormone secretion. Moreover, phosphotyrosine phosphatases (PTPs) are activated by SST. PTPs can activate two different pathways: the first shows as consequence cytostatic effects by the inhibition of the Mitogen Activated Protein Kinase, the second leds to the apoptosis activation, having as last event cell death[85,7] (Figure 3).

Because SST is involved in the inhibition of hormone secretion and brings to cytostatic or cytotoxic effects and because SSTRs are over-expressed in different types of tumors, SST and it activated pathways are the most studied processes for cancer treatment and diagnosis.

## 2.3 Somatostatin and its analogues.

### 2.3.1 Agonists.

When a SST-analogue with an agonist behaviour binds to it specific SSTR subtype, G-protein are activated by phosphorilation through protein kinases

A/C and G-protein coupled receptors (GPCR) kinases and the mechanism that derives is the internalisation of the SSTR-agonist complex.

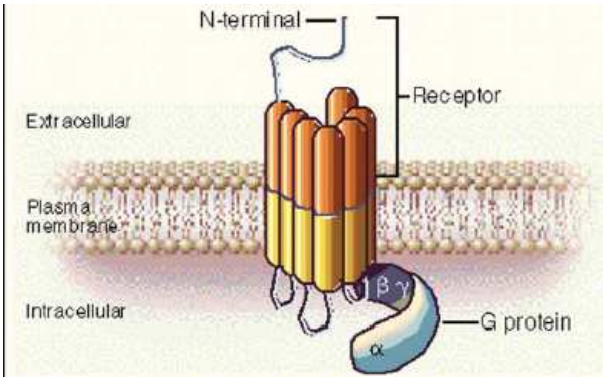


**Figure 2**: G-protein coupled receptor[94].

Internalisation occurs with the formation of clathrin-coated pits (involving β-arrestins). The internalised complex is then channel to endosomes, where dephosphorilation occurs. Finally, the receptors are recycled and go back to the membrane as functional receptors[28] (Figure 4). GPCR down-regulation results from lysozomal degradation of intracellular receptors, this led to a decrease of mRNA and protein synthesis.

Due to its actions, SST started to be studied in particular for the therapy of SSTR-expressing tumors. Native SST has a very short half life in human serum (about 3 minutes), because it is rapidly attacked and degraded by endogen reducing agent as glutathione oxidase, thioredoxin reductase or basic and nucleophilic agents, thus preventing it application to the clinic. In order to get over this difficulty, SST-analogs with different affinity to each SSTR subtypes and with different behaviour were synthesized.

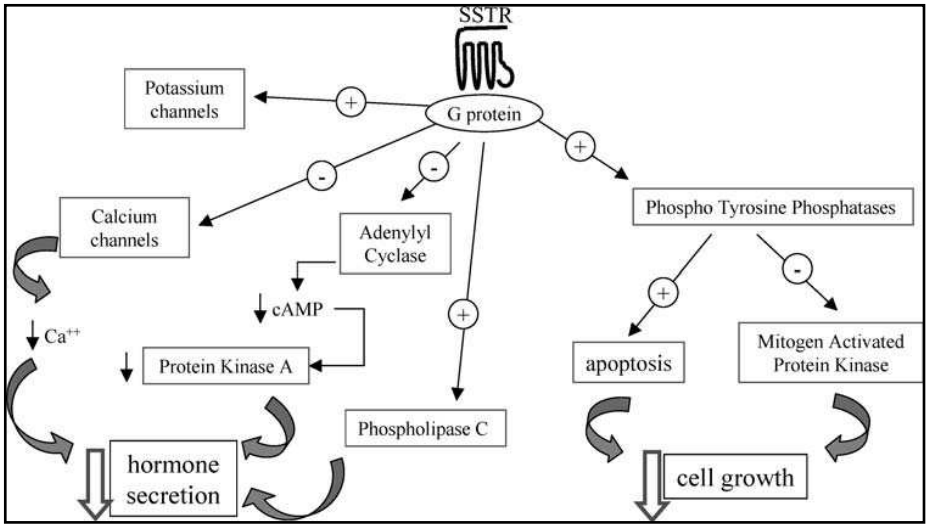


**Figure 3**: SST mechanism of actions[92].

The first and well known SST-analogue is Octreotide, also named SMS 201-995 or Sandostatine®. It is a cyclic octapeptide that maintain the SST pharmacophore together with a protection against degradation, that are represented by the presence of a D-Phe residue at N-terminus together with an alcoholic residue (Thr-ol) at C-terminus. Metabolic stability was given by the presence of a disulphide bridge between $Cys^2$-$Cys^7$ (Figure 5). Octreotide has an half life of 117 minutes in human serum, a great affinity for SSTR-2 and a moderate affinity for SSTR-3/5 (Table 1).

Later, new peptides with different affinity profiles and different behaviour were synthesised, but Octreotide is still considered the milestone in the SST-analogues history. For example, other analogues that are now in clinical trials are Lanreotide and Vapreotide but, even in these cases the main limiting factor remains the affinity to each SSTR subtypes. Because SST has a large spectra of action and in particular for it antisecretory action, the potential of SST analogues in cancer treatment is very high, especially for

those tumors such as pituitary tumors, gastrointestinal tract, acromegaly, prevention and treatment of pancreatic surgery complications.

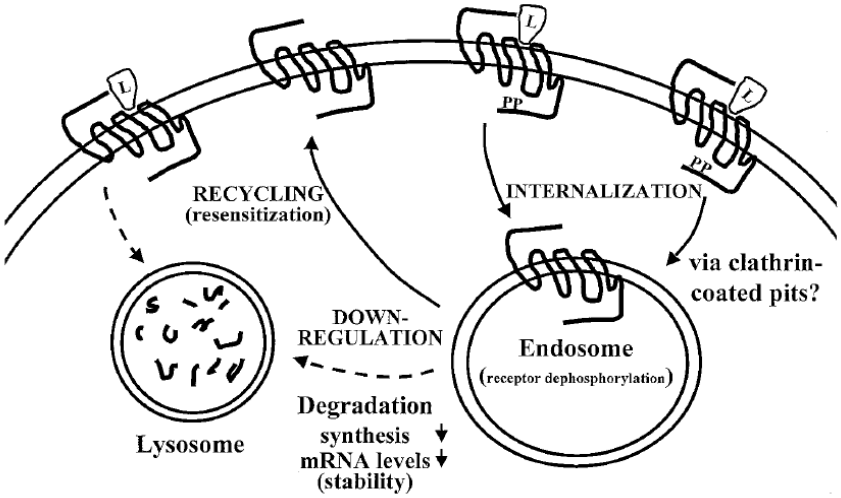


**Figure 4**: Rapresentation of intracellular routing of GPCRs after agonist activation (L= ligand, PP= phosphate group)[28].

Even if these drugs are very promising, an important problem to underline is the typical behaviour of SSTRs. In fact, this receptors have the particularity to create homo- and heterodimers with the receptors of other system (dopamininergic and opioid receptors), becoming very difficult to predict the therapeutic potential of SST-analogues.

| ***Compound*** | ***hsstr1*** | ***hsstr2*** | ***hsstr3*** | ***hsstr4*** | ***hsstr5*** |
|---|---|---|---|---|---|
| SS-14 | 1.1 | 1.3 | 1.6 | 0.53 | 0.9 |
| SS-28 | 2.2 | 4.1 | 6.1 | 1.1 | 0.07 |
| Octreotide | > 1000 | 2.1 | 4.4 | > 1000 | 5.6 |
| Lanreotide | > 1000 | 1.8 | 43 | 66 | 0.62 |
| Vapreotide | > 1000 | 5.4 | 31 | 45 | 0.7 |

**Table 1**. Binding affinities (Ki, nM) to hSSTR of clinically used SST-analogues[86].

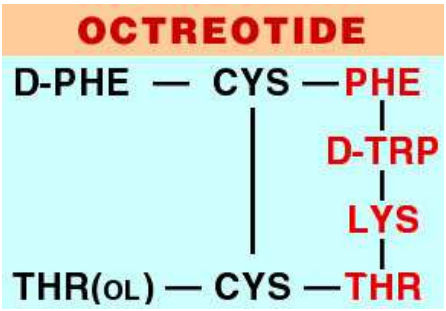


**Figure 5**: Octreotide. Pharmacophore corresponds to the red aminoacids.

## 2.4 Somatostatin analogues and cancer.

Due to it antisecretory activity, the therapeutic potential of SST in cancer treatment is multiple.

Different neoplasms express a particular SSTR or co-express more than one SSTR subtypes. This was abundantly studied during the last twenty years. For example, pituitary adenomas express SSTR-2 and -5, receptors that are important in inhibiting the excessive GH secretion in acromegaly. Since GH stimulates production of IGF-I, that has been implicated in promoting cancer[87], SST-analogues may retard additional cancers by decreasing systemic GH/IGF levels[88].

Another important mechanism of anti-neoplastic action of these drugs appears to be the inhibition of neoangiogenesis.

Angiogenesis is a fundamental process in the context of tumour growth, and one of the main factors involved in the appearance of new tumour vessels is vascular endothelial growth factor (VEGF). SST-analogues inhibit the production and secretion of many angiogenic factors[89]. It has been demonstrated that octreotide induced inhibition of angiogenesis by a process that is G-protein, calcium- and cAMP dependent and is protein protein-

kinase C (PKC) and PTP independent[90]. SSTRs expression has been demonstrated in peritumoral vessels in different tumour types, and it appears to be unrelated to the receptor expression in the tumour cells[24]. SSTR2 is expressed when the endothelial cells begin growing[91]. In fact, SSTR2 gene is expressed on proliferating angiogenic vessels. These data were confirmed by immunohistochemistry and *in vivo* scintigraphy. This is the reason, because SSTR2 may be a specific target for anti-angiogenic therapy with SSTR2-binding SST conjugated to radioisotopes (section 2.5) or cytotoxic agents.

Preclinical studies on the potentiality of SST analogues in inhibiting angiogenesis were performed in different experimental models, including the chicken chorioallantoic membrane model, the human umbilical vein endothelial cell proliferation model and the human placental vein angiogenesis model.

Recent studies have focused on SSTRs signalling and its effects on cell growth, because it is recognized that SST has activity as endogenous antiproliferative agent in many different experimental tumor models both *in vivo* and *in vitro*[92]. However, these effects, that are highly significant in preclinical study, become much more questionable when the data are translated to clinical trials, so that the research is still moving further and a significant progress is doing in understanding the mechanism by witch SSTR activation may lead to cytostatic or apoptotic effects. In particular, it is now accepted that, the main transduction system involved in the antiproliferative activity of SST is represented by the activation of a subset of phosphotyrosine phosphotases[92,92].

Therefore, the effects of SST on tumor cell growth may take place at different levels[93]: directly blocking the cell cycle progression through the binding to SSTRs expressed on cell and the activation of PTPs, and

indirectly through the modulation of tumor growth mediated by the inhibition of the production of GF, or via an antiangiogenic effect.

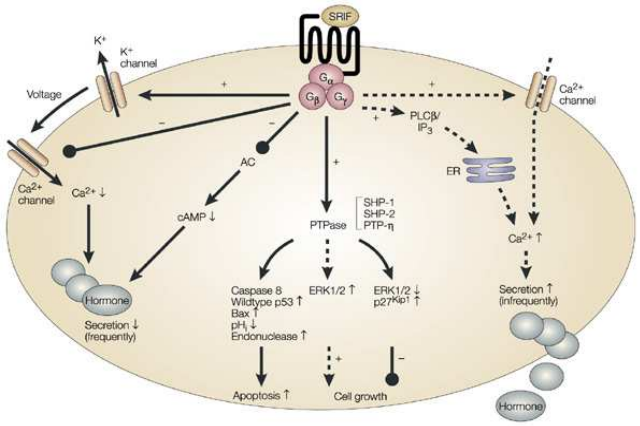


**Figure 6**: Somatostatin receptors characteristics[94].

Frequently, the activation of SSTRs causes cytostatic effects, with cell's block in the G1 phase. The role of SST as an endogenous regulator of cell cycle is a recognised activity and, using different *in vitro* and *in vivo* experimental models, all the five SSTR subtypes were reported to induce arrest of cell proliferation[94] or induce apoptosis[88] too.

Different SSTRs (SSTR1, SSTR2, SSTR4 and SSTR5) have been implicated *in vitro* in the G1–G0 cell cycle blockade, while the apoptotic effect of SST being mediated through SSTR3 and less through SSTR2.

SSTR-3 was shown to increase wild type p53 through a dephosphorylation-dependent conformational change and to induce Bax, but not p21, in apoptosis caused by octreotide treatment of Chinese Hamster Ovary cancer (CHO) cell line stably transfected with human-SSTRs and MCF-7 human breast adenocarcinoma cells[95], where transient G2/M blockade and apoptosis were demonstrated[96]. In these cells, octreotide had cytotoxic effects leading to apoptosis, with a rapid time-dependent induction of wild-type p53.

In human pancreatic adenocarcinoma, it was demonstrate that, during the tumoral progression, the cells lose the ability to express SSTR2 but, reintroducing this receptor into the pancreatic cancer cells by stable expression, leads to a constitutive activation of the SSTR2 gene and evokes a negative feedback loop, inhibiting cell proliferation. This may suggest that SSTR2 gene transfer might be considered as a possible novel therapy for pancreatic cancer [97] (Figure 6; Table 2).

| | SSTR1 | SSTR2 | SSTR3 | SSTR4 | SSTR5 |
|---|---|---|---|---|---|
| Chromosome | 14q13 | 17q24 | 22q13 | 20p11 | 16p13.3 |
| Aminoacid sequences | 391 | 369 | 418 | 388 | 363 |
| MAPK modulation | + | + | + | + | + |
| Signalling via PTP | ↑ | ↑ | ↑ | ↑ | ↑ |
| Effect on cAMP | ↓ | ↓ | ↓ | ↓ | ↓ |
| Functions | ↓Angiogenesis ↑cell cycle arrest | ↓hormonal secretion ↑cell cycle arrest | ↑apoptosis | ↑cell cycle arrest | ↓hormonal secretion ↑cell cycle arrest |

**Table 2**: Somatostatin receptors characteristics (chromosomal localisation of the genes encoding the five SSTR subtypes; aminoacids structure; G-protein coupling and activation; effect on cAMP; signalling via tyrosine phosphatases and receptor-specific functions)[98].

Even if, the cytotoxic and cytostatic effects of SST analogues were abundantly studied *in vitro,* currently, no consistent results were proved in patients to inhibit cell proliferation or metastasis in NETs. In fact, treatment with SST-analogues has produced variable results in clinical practice especially when used as single agent. Poor results were seen with rapidly progressive tumors, with high proliferation capacity despite the presence of SSTRs[99]. Conversely, well-differentiated tumors such as mid-gut carcinoids respond well, with stabilization of tumor growth over many years.

What is well established is that SST can decrease in tumor growth from indirect effects, through suppression of synthesis and secretion of GFs and

some hormones (insulin, prolactin, IGF-1, EGF, TGF-α, gastrin, cholecystokinin and GH). An important example is constituted by IGF-1, that plays as modulator of many neoplasms, because SST analogues suppress the GH-IGF-1 axis by both central and peripheral mechanisms.

Experimental studies of combinations of octreotide with antimitotic drugs resulted in slightly additive actions[100,101].

Furthermore, somatostatin analogs have also been used as carriers to deliver cytotoxic agents to cancer cells.

## 2.5 Radiolabeled Somatostatin-analogs.

The presence of SSTRs in different neoplasm can be exploited, not only in long term therapy with not-cytotoxic SST-analogs, but also in tumor diagnosis and therapy with radioactive analogues. The use radiolabeled SST analogues derives from the necessity to obtain consistent inhibition of cell proliferation or metastasis in NETs, exploiting cytotoxic effects due to radiation.

Thus, basic knowledge of SSTR subtype profiles in different neoplasm, the affinity profile, binding/internalization of SST analogues-carried radionuclides features are critical for the evaluation of the potential usefulness of receptor-mediated radiotherapy. The uptake of radiolabeled SST-analogues depends on the number of SSTR on the cell membrane, on the internalization rate and on the of the recycling time and mass of the radiolabeled peptide.

In nuclear medicine, two are the techniques for diagnosis using radionuclides: γ-scintigraphy and positron emission tomography (PET). The main differences between the two technologies consisting in the different emission spectra of the radionuclides exploited. In fact, it is necessary to

adopt radiopharmaceuticals containing a radionuclides that emits γ-radiation with an energy between 100-250 KeV in γ-scintigraphy and the required instrumentations are γ camera and SPECT camera. PET camera requires pharmaceuticals radiolabeled with $\beta^+$ emitting radionuclides (positron emission) and a PET or PET-CT camera.

The first radiolabeled SST-analogue was [$^{123}$I-Tyr$^3$]-octreotide, a radiopharmaceutical with γ-emission[102]. The radiopeptide was used for *in vivo* localisation of tumors, but although the pharmacological profile was optimal with a very high SSTR2 affinity ($IC_{50}$= 2.0±0.7 nM) and a very high internalisation rate in tumoral cells, the radiopharmaceutical was turned out be useful as a diagnostic tool. This was due to the lipophilic feature of [$^{123}$I-Tyr$^3$]-octreotide, that bring to an hepatobiliary exctretion, with the consequence that abdomen imaging results with low sensitivity.

Subsequently, a first chelator was united to octreotide: DTPA (Diethylentriaminepentaacetic acid). This chelator allows the radiolabelling with 111-Indium, giving a hydrophilic feature to the radiopeptide and a renal excretion. $^{111}$In-DTPA-Octreotide gave a better biodistribution profile, even if affinity for SSTR2 was reduced ($IC_{50}$= 22±3.6 nM). $^{111}$In-DTPA-Octreotide was the first commercialized radiopeptide for diagnostic imaging in nuclear medicine (Octreoscan®, $^{111}$In-pentereotide, Millinckrodt Med., St. Louis, MO, USA).

Subsequently, new strategies were developed and research was moved to find new solutions to allow the radiolabelling of SST-analogues with other radionucides, both for γ-scintigraphy and PET.

Particularly, DTPA was substituted by HYNIC ( 2-hydrazinonicotinic acid) to be possible radiolabeling with $^{99m}$Tc. This radiometal has a very low cost production and a short half life (6 h). At moment, there are two different successful $^{99m}$Tc-radiolabeled SST-analogue: these radioconjugates

demonstrated good results if compared to Octreoscan®. These are $^{99m}$Tc-$N_4$-Tyr$^3$-Octreotide and $^{99m}$Tc-HYNIC-Tyr$^3$-Octreotide (HYNIC-TOC). Tyr$^3$-Octreotide is synthesised in a more recent times compared to octreotide and presents the octreotide skeleton, but of the third aminoacid is a Tyrosine instead of a Phenilalanine (Phe is replaced by a Tyr).

SST-analogues were radiolabeled with $^{18}$F too. In this case, inconveniences are a rapid washout of the radiopeptide, an high liver uptake and a consequent not clear imaging of the abdominal area[103]. Another radiometal with $\beta^+$ emission is $^{64}$Cu, that is also used for SST-analogues radiolabelling and from preclinical data, particularly biodistribution profile on animal model seems favourable[104].

The introduction of the macrocyclic chelator DOTA (1,4,10-tetraazacyclododecane-1,4,7,10-tetraacetic acid) gave advances in this technology. The obtained metal complex is kinetically and thermodynamically stable. This radiometal is encapsulated and embedded inside the macrocyclic cage which protects it from the attack of competing ligands present in the human tissues and the body fluids. DOTA chelator makes possible the radiolabelling with different radiometals, such as: $^{111}$In, $^{90/86}$Y, $^{177}$Lu and $^{66/67/68}$Ga. $^{68}$Ga-Tyr$^3$-octreotide ($^{68}$Ga-DOTATOC) is a very successful radiopeptide for tumor imaging with PET scan, in fact the radiopharmaceutical offers a very high quality imaging and a very high tumor-to-background ratio[105,104].

Consequence of peptide receptor mediated scintigraphy was peptide receptor mediated radionuclide therapy (PRRT). To have a successful PRRT, four requirements are necessary. These are:

- The number of receptors on tumoral cells have to be high in number.
- The radiopeptide needs to be internalised in tumoral cells.

- The radionuclides have to emit radiations with an high linear energy transfer (LET), in order to destroy the tumor tissue.
- The whole metal-chelator-peptide complex must have suitable pharmacokinetics.

There are three types of therapeutic radionuclides: α-emitters, β-emitters and Auger-electron emitters, each one with different range of energy deposition and LET properties (Figure 7). Radionuclides with β emission are the most used in the current clinical practise for therapeutic applications. The advantage for β–emitters is that it is not required to target all the tumoral cells for their killing (crossfire effect, low LET). There are different type of β-emitters radionuclides and are classified considering their energy of emission. So, there are β-emitters radionuclides with a low range (mean range <200µm, as $^{177}$Lu), with a medium range (mean range between 200µm and less than 1 mm, as $^{67}$Cu, $^{153}$Sm) and high range (mean range >1 mm, as $^{90}$Y). Moreover, for those cases where γ-emissions are present too, biodistribution profile is reproducible, for example $^{177}$Lu has a γ-emissions (160-202 KeV), while Y-90 is a pure $\beta^-$emitter.

α-emitters particles emits with an high LET over a path length of 3-4 cells diameters.

Auger-electron emitters have an electron energy between 10 KeV and several eV. This type of radionuclides have a very short effect range (several nanometers) and high toxicity, giving them ideal for small cluster metastatic cells therapy.

The first widely used radiolabelled SST-analogues for PRRT was $^{90}$Y-DOTA-Tyr$^3$-octreotide ($^{90}$Y-DOTATOC)[106,107]. Studies have demonstrated that $^{90}$Y-DOTA-Tyr$^3$-octreotide is successful for the therapy of metastatic

NETs, in particular in pancreatic tumors and carcinoids, but some evidences are described for other NETs too[108].

Another radiopharmaceutical used for PRRT is DOTA-Tyr$^3$-Thr$^8$-octreotide (DOTATATE), which differs from DOTA-Tyr$^3$-octreotide by a aminoacidic modification in the aminoacid number 8 (the alcoholic molecule was take off: Thr (ol) became Thr) (Figure 8). The peptide retains high affinity for human SSTR2 as demonstrated by $Y^{III}$-DOTATATE binding studies (7-fold higher compared to $Y^{III}$-DOTATOC) (Table 3).

Despite this higher affinity for SSTR2, biodistribution profiles of $^{111}$In-DOTATOC and $^{111}$In-DOTATATE are very similar. Further, preclinical studies on nude mice bearing SSTR2-xenograft tumor demonstrated that $^{177}$Lu- has performed better compared to $^{90}$Y in small or medium tumors. This behaviour is related to Lutetium-177 maximum tissue range of 2 mm compared to 11 mm of Yttrium-90. Additionally, $^{177}$Lu emits γ-radiation, giving the possibility to obtain the biodistribution profile after the PRRT.

| **Compound** | **hSSTR1** | **hSSTR2** | **hSSTR 3** | **hSSTR4** | **hSSTR5** |
|---|---|---|---|---|---|
| SS-28 | 5.2±0.3 | 2.7±0.3 | 7.7±0.9 | 5.6±0.4 | 4.0±0.3 |
| InIII-DTPA-octreotide | > 10,000 | 22±3.6 | 182±13 | >1,000 | 237±52 |
| YIII-DOTA-OC | >10,000 | 20±2 | 27±8 | >10,000 | 57±22 |
| YIII-DOTA-TOC | >10,000 | 11±1.7 | 389±135 | >10,000 | 114±29 |
| YIII-DOTA-TATE | >10,000 | 1.6±0.4 | >1,000 | 523±239 | 187±50 |
| YIII-DOTA-Lanreotide | >10,000 | 23±5 | 290±105 | >10,000 | 16±3.4 |
| YIII-DOTA-Vapreotide | >10,000 | 12±2 | 102±25 | 778±225 | 20±2.3 |

**Table 3:**Affinity profiles for human SSTR1-5 of a series of Somatostatin analogues (values are expressed as $IC_{50} \pm$ SEM, in nM)[109].

Summarizing, it is important to underline that when a chelator is added to the peptide, some changing in affinities profile are obtained. For example, it can be present a loss of affinity for a particular subtype receptor, especially for

SSTR5, but also for SSTR3 and SSTR2. Not only, changing in affinity profiles are obtained when a metal is present and a particular metal instead of another.

Although the *in vivo* metabolism, excretion pathway and retention times of a molecule are important parameters for its evaluation as a new tracer for diagnosis or therapy, there is no doubt that the *in vitro* characterization of the receptor binding affinity of such a molecule is crucial information, particularly nowadays when several studies on the receptor expression pattern on tumors are available.

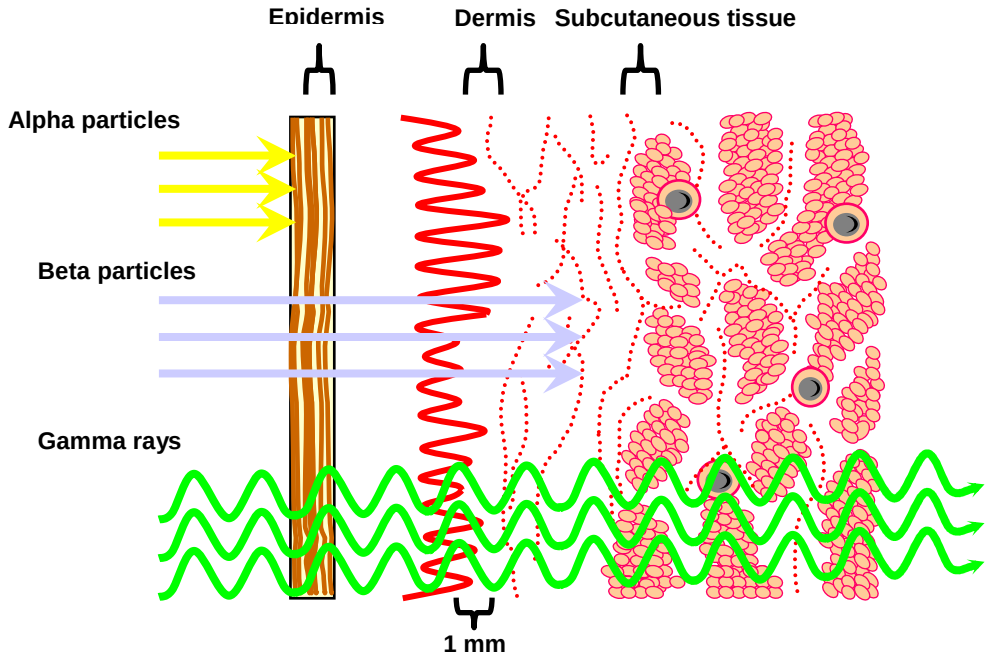


**Figure 7**: Penetration of Particulate and Electromagnetic Radiation.

Therefore, the conclusion from the informations presented here is that the efficacy of the currently used radiolabeled somatostatin analogues derives mainly from their moderate to high affinity for SSTR2, the receptor with the widest distribution among the SSTR family.

Having complex structures, in which every component influences the biological efficacy *in vivo,* it is still a challenge to find the best metal-chelator-SST analogue structure with not only suitable pharmacological properties, but also with optimal pharmacokinetics and pharmacodynamics.

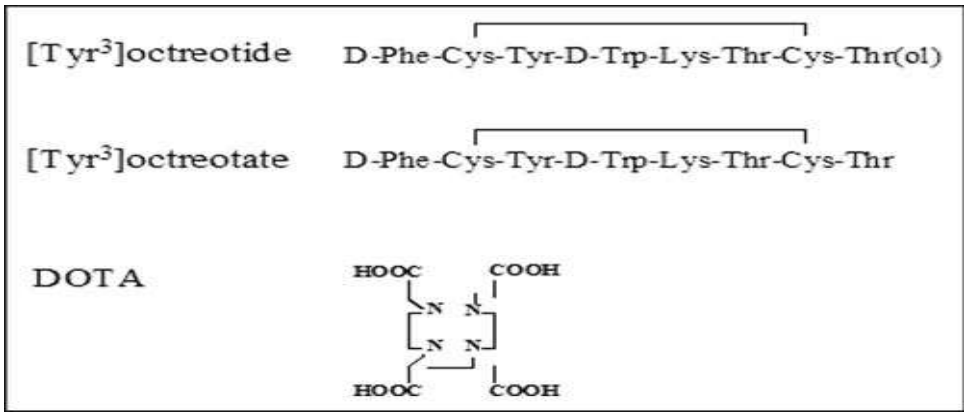


**Figure 8**: Structures of the somatostatin analogues Tyr[3]-octreotide and Tyr[3]-octreotate and of the chelator DOTA[110].

# 3 Strategies to improve pharmacological profile of radiolabeled Somatostatin analogues.

## 3.1 Characteristics of Somatostatin analogues for Nuclear Medicine.

Summarizing, the factors limiting therapeutic efficacy of SST analogues are their selectivity for a particular SSTR, requiring a precise determination of receptor subtypes expression in tumor tissue before therapy and their partial answer in therapeutic protocols used in clinic until now, consisting in their antisecretory activity. On the other hand, native SST with great affinity for all five SST receptors, are not practise in clinical, because SST has a short

plasma half-life (1–3 minutes in humans), giving necessary continues infusion on treated patients.

Mainly for this reasons and for the unsuccessful results in therapeutic protocols in the last years oncologic research was devoted to the development and synthesis of new pharmaceuticals which, once radiolabeled and injected *in vivo*, can be used in for imaging and therapy of tumours.

For this purpose, labelled molecules must possess high selectivity towards tumour cells or tissues to reach efficient targeting activity.

At moment, in nuclear medicine the current SST analogues used both for diagnosis and therapy shows good affinity for SSTR2 and a moderate affinity for SSTR3-5 (Table 4).

SST-14 served as model for all the analogues synthesized over the years and all the radiolabeled somatostatin based compounds used in clinical applications are derivates of octreotide. Octreotide have a critical position between two aminoacids, that is maintained from the native molecule and, if it is replaced, it could give modification in the biological properties of the molecule. This sequence corresponds to the $Lys^5$- D-$Thr^6$ where a β-turn is present. The main modifications present in the SST analogues in clinical practise are: a changing in position 3 (Phe >Tyr) for vapreotide, lanreotide and TOC and a substitution of the sixth aminoacid (Thr>Val) for lanreotide and vapreotide.

Other modifications could are present at C-terminus and at N-terminus of the peptide and of course each of these modifications induce changing in the affinity profiles (Table 4).

Even if some important results are obtained by PRRT, new SST analogues with high affinity for a particular SSTR subtype as SSTR3 and SSTR5 or a pan-SST analogue (analogues that possess high affinity for all the subtype

receptors) are required, so that PRRT with maximal therapeutic effects can be performed on patients.

| **Compound** | **hSSTR 1** | **hSSTR 2** | **hSSTR 3** | **hSSTR 4** | **hSSTR 5** |
|---|---|---|---|---|---|
| SST-28 | 5.2±0.3 | 2.7±0.3 | 7.7±0.9 | 5.6±0.4 | 4.0±0.3 |
| $In^{III}$-DTPA-OC | > 10,000 | 22±3.6 | 182±13 | > 1,000 | 237±52 |
| $Y^{III}$-DOTA-OC | >10,000 | 20±2 | 27±8 | >10,000 | 57±22 |
| $Y^{III}$-DOTA-TOC | >10,000 | 11±1.7 | 389±135 | >10,000 | 114±29 |
| $Y^{III}$-DOTA-TATE | >10,000 | 1.6±0.4 | >1,000 | 523±239 | 187±50 |
| $Y^{III}$-DOTA-Lanreotide | >10,000 | 23±5 | 290±105 | >10,000 | 16±3.4 |
| $Y^{III}$-DOTA-Vapreotide | >10,000 | 12±2 | 102±25 | 778±225 | 20±2.3 |

**Table 4:** Affinity profiles for human SSTR1-5 of a series of somatostatin analogues (values are expressed as $IC_{50}$ ± SEM, in nM)[109].

## 3.2 Modification of pharmacokinetics/pharmacodynamics of radiolabeled Somatostatin analogues.

Affinity is a crucial parameter for a new peptide development, in fact this parameter corresponds to the tendency of a drug to bind to a binding site including specific receptor. Affinity can be evaluated at equilibrium by the affinity or association constant (sometimes given the symbol K), which is the reciprocal of the dissociation constant ($K_D$), or it can be measured in $pD_2$ units, that corresponds to the negative logarithm of the concentration of the agonist that produce half of the maximal response.

So, the molar concentration of a drug inducing 50% of the maximal response is considered the affinity between a drug to it proper receptor ($IC_{50}$) and it is expressed as the negative logarithm of the concentration of the agonist that produce half of the maximal response.

Affinity studies are the first step of a very long study, if a new drug is the target of the research.

If affinity profile is favourable, the next step will be performed. In nuclear medicine, it is usual that the new peptide is linked to a chelator molecule that allows the radiolabeling with different radiometal so, it is important to perform affinity assay even after the chelator linking, because this molecule can induce some modifications in binding assays results. After this passage, radiolabeling and stability tests are to be performed. Another important step consisting in the measurement of human serum stability and *in vitro* assays on an adapt cell line. This last step is important to establish an eventually biological effect of the new radiopeptide. After this phase, experiments will be performed on animal models. Objective of this phase is to establish the biodistribution profile of the radiopharmaceutical, if the radiopharmaceutical goes to it target, the washout, if there are any secondary effects (kidney burning, for example).

After all these evaluations, a clinical phase on patient could be started. Of course, it could be that a very promising radiopharmaceutical from preclinical data gives unlucky results on men, infect, *in vivo* studies on animals can not predict the drug behaviour in humans. This is the case of $^{123}$I-[3-iodo-Tyr$^{3}$]-octreotide where, despite the very spectacular first results, the radiopharmaceutical was abandoned, because of the high hepatobiliary excretion, with the consequence that abdomen imaging results with low sensitivity.

There are a lot of different SST analogues, each one with a different affinity and different behaviour and, for researchers, the purpose still remains to design new pharmaceuticals with a more elective action, a better affinity for a particular SSTR subtype and a prolonged action replacing the others in the current trade.

## 3.3 Modulation in hydrophilicity/lipophilicity.

Clearance refers to the volume of blood or plasma cleared of a drug in a unit time. It is defined as the product of the volume of distribution rate constant and only unbound proteins are available for clearance. Physiologic excretion pathway of the drugs are mainly through liver or kidney, it depend by the characteristic of the pharmaceutical.

For radiopharmaceuticals, the excretion pathway is of crucial importance for both the diagnostic performances (high tumor/background ratios, thus signal intensity in diagnostic by PET or SPECT) and low toxicity profile in therapy. Regarding SST analogues, particularly the DOTA chelated analogues, the hydrophilic characteristic of these peptides determine a predominant renal clearance making the kidney the dose limiting toxicity organ for PRRT. For this reason, efforts are directed to increase lypophilicity of the compounds. Of course, these modifications have not to influence the affinity profile.

The current radiolabeled SST analogues, $^{111}$In/$^{90}$Y-DOTA-octreotide and octreotide derivates demonstrated an increased metabolic clearance with a gallbladder accumulation. The same was observed in $^{68}$Ga-DOTA-octreotide derivates, where the abdominal uptake did not demonstrate any refinement.

This problem can be crossed adding an hydrophilic spacer, hoping that pharmacological performance will be maintained.

## 3.4 Lowering the kidney uptake .

The treatment of patients with SSTR positive tumours with peptide receptor radionuclide therapy (PRRT) has with no doubt beneficial effects. One of the

limits of this therapy is represented by kidney burning. In fact, the radiolabelled peptides are rapidly cleared via the glomeruli in the kidneys into the urine, but a low percentage is reabsorbed and retained in the cortical proximal tubules. After glomerular filtration a fraction of the administered peptides is internalized via endocytic receptors; megalin is responsible to this process. Transfer of the radiopeptides to the lysosomes is followed by degradation of the peptide, after which aminoacid chelate conjugates are trapped in the lysosomes of the tubular cells, delivering a high radiation dose to the renal cortex during PRRT. In PRRT, the maximum tolerated dose in patients is not exactly known, but dosimetric studies applying the principle of the biological equivalent dose (correcting for the effect of dose fractionation) suggest that a dose of about 37 Gy is the threshold for development of kidney toxicity. This threshold is lower when risk factors for development of renal damage exist: age over 60 years, hypertension, diabetes mellitus and previous chemotherapy, but the upper limit for kidney safety is fixed to 27 Gy[111].

In Erasmus Medical Centre in Rotterdam, co-infusion of lysine and arginine (Lys/Arg) has become a standard procedure during PRRT with $^{177}$Lu- or $^{90}$Y-labelled somatostatin analogues, reducing the renal retention of the radiopeptides by approximately 35%[112].

## 3.5 Targeting the cell nucleus.

To have a successful PRRT, there are some parameters that a clinician have to consider. Of course the presence of an high density of SSTRs on tumoral cells is the first one, but it is not the unique. In fact it has to consider if the radiopeptide has a very high affinity for the expressed SSTR subtype and if the SSTR are functional. After these considerations, others important

reflections have to be done: is the receptor-peptide internalised into the tumoral cells? And in case of affirmative answer: how long is the radiopharmaceutical retention time in cells? Retention time is a very crucial parameter, because if it is very long, the radiopharmaceutical have a maximal therapeutic effect. In PRRT, the radiometals mainly used are $^{90}Y$ and $^{177}Lu$, these shows respectively an intermediate and high energy, making fruitful a therapy on medium or large tumor diameter, where the cytotoxic effect is due to the cross-fire effect. The problem is that β-emitters do not show any effectiveness on small metastasis cell cluster, but the problem can be easily surpassed using radiometals with different characteristics. The ideal radioemitters are Auger-electron emitters, because of their high toxicity and short effect range (several nanometers).

There are some radionuclides that emits Auger electrons (Table 5), some of them are currently used in the routine clinical practise. Auger electron emitters, inducing DNA damage by indirect mechanism, led to cell death. Moreover, a prolonged retention of the radiopeptide in the target cells will bring to an unquestionable success of PRRT.

Auger-electron emitter antibodies conjugates demonstrated positive results for the therapy of different pathologies, in particular for B-cell lymphomas[113] and some preclinicals studies were also started for SST analogues and the results seem encouraging.

Finally, it is important to point the attention to those SST analogues that demonstrated an antagonist behaviour, where their importance in PRRT seems to be controversial.

The rationale is that agonists, after high-affinity binding to the receptor, usually trigger internalization of the ligand–receptor complex[114]. The internalization process is the basis for an efficient accumulation of the radioligand in a cell over time and it has been considered a crucial step in the

process of *in vivo* receptor targeting with radiolabeled peptides. But there are few information about those SST analogues that not demonstrated the ability to trigger receptor internalization. This molecule shows an antagonist behaviour, stably binding to their specific SSTR subtypes, but not activating any biological answer and this is the reason because antagonists were not considered in for therapy. However, antagonists may have characteristics other than those related to internalization that may make their radiolabeled derivatives suitable tools for in vivo receptor targeting[115].

| **Radionuclide** | **Half-life** | **Auger yield** | **Auger energy (keV)** |
|---|---|---|---|
| $^{51}$Cr | 27.7 d | 5.4 | 3.65 |
| $^{55}$Fe | 2.73 d | 5.1 | 4.17 |
| $^{67}$Ga | 3.26 d | 4.7 | 6.26 |
| $^{75}$Se | 120 d | 7.4 | 5.74 |
| $^{99m}$Tc | 6.01 h | 4.0 | 0.89 |
| $^{111}$In | 2.8 d | 14.7 | 6.75 |
| $^{113m}$In | 1.66 h | 4.3 | 2.04 |
| $^{115m}$In | 4.5 d | 6.1 | 2.84 |
| $^{123}$I | 13.2 h | 14.9 | 7.42 |
| $^{125}$I | 60.1 d | 24.9 | 12.24 |
| $^{193m}$Pt | 4.33 d | 26.4 | 10.35 |
| $^{195m}$Pt | 4.02 d | 32.8 | 22.52 |
| $^{203}$Pb | 2.16 d | 23.3 | 11.63 |

**Table 5:** Characteristics of some Auger-emitting radionuclides[116] . The Auger yield is the mean number of Auger and Coster-Kronig electrons emitted per decay. The Auger energy is the average total kinetic energy of Auger and Coster-Kronig electrons emitted per decay.

Most relevant is the *in vitro* evidence that, in certain circumstances, antagonist radioligands may label an higher number of receptor-binding sites than agonist radioligands, in fact Ginj et al.[115] demonstrated that adequately labelled SSTR2-3 antagonists, even though they do not internalize, may be useful radioligands to target tumors *in vivo*. More importantly, it also shows

that antagonists may be even better candidates to target tumors than agonists with comparable binding characteristics because the radiopeptide remains stably bound to it proper receptor both *in vitro* and *in vivo* experiments.

## 3.6 Understanding the post-endocytic pathway of SSRs.

When a G-protein coupled receptor is activated, the activated molecular mechanism requires some minutes because the signalling transduction starts. The processes of internalization and desensitization are adaptive mechanisms that prevent persistent receptor stimulation from producing detrimental cellular effects. Internalization may also play a role in receptor resensitization. A critical first step in both G-protein coupled receptors internalization and desensitization is believed to be receptor phosphorylation by G-protein kinases and second messenger activated kinases. In case of SSTR2, it was demonstrated that there are some aminoacids at carboxyl-terminus that are phophorylated after the agonist-receptor binding. Then phosphorylated receptors bind regulatory proteins called arrestins, which inhibit further signaling by blocking receptor-G protein interaction[117,118].
Several studies have proved the phosphorylation of different SSTR subtypes upon agonist activation[119,120,121]. Special attention has been given to SSTR2 subtype[122,123] because, due to its presence in a wide range of tumors, modulation of SSTR2 receptor function is likely to have important therapeutic consequences and possibly may be exploited to improve SSTR2 receptor-mediated radioligand internalization. Therefore, elucidation of early events, which occur after exposure to agonist as well as heterologous hormones, may provide new strategies to enhance the clinical utility of SSTR2 receptor-target drug.

# AIMS OF THE PROJECT

Aim of the study is to evaluate new SST-analogues recently prepared through a ring-closing metathesis of the on-resin linear octapeptide carrying two allil-glycine in the place of the corresponding cysteine residues. These molecules keep the same sequence of the parent octreotide with some modifications. These new molecules were developed and synthesized in Laboratory of Peptides and Proteins, Chemistry and Biology (University of Florence).

In order to evaluate the affinity of new compounds to the different subtypes of human SSTRs, the radioligand binding assays were performed. First results of binding assays gave the possibility to focus the attention on two of these SST analogues and in particular for those that demonstrated high affinity for SSTR2, SSTR5 or both of them. These two SST analogues, that were called Peptide 1 and Peptide 2. After their coupling with DOTA, binding profile was re-tested. DOTA-Peptide 1 was chosen for this study since the chelation with DOTA does not altered its affinity to SSTR2 ($IC_{50}$ was even increased) while affinity for SSTR5 was lost. DOTA-Peptide 2 lost it affinity for SSTR5.

The program takes advantage of synergic research strategies addressing pharmacological, biological, radiochemical, radiopharmacological and radiodosimetrical issues with the final objective to develop new suitable radiolabelled octreotide analogues for PRRT and for *in vivo* imaging.

The project is focused on the evaluation of the new analogue after labelling with radiometals ($^{177}$Lu, $^{111}$In). Internalisation and cellular retention on cell lines expressing SSTR2 and of the biodistribution profiles are performed.

The dynamic binding of the radiolabelled analogue was evaluated real-time by a new methodology, the LigandTracer® for interaction analysis.

Immunofluorescence studies were performed, treating the cells with a fixed concentration of the SST analogue for established times to visualize the intracellular localization of the SSTR-peptide complex.

Finally, the proapoptotic effect of the SST analogue was studied performing TUNEL assay.

# MATERIALS AND METHODS

## 1 Peptides Synthesis.

Peptide was synthesised in a Teflon reactor fitted with a polystyrene porous frit. Peptide was prepared using the general Fmoc-SPPS strategy on pre-swelled H–L-Thr(*t*Bu)–ol–2–chlorotrityl resin (0.5 mmol/g). Couplings were performed by adding two equivalents of protected amino acid activated by HATU and four equivalents NMM in DMF, stirring for 45 minutes for each coupling and monitoring by the qualitative ninhydrin (Kaiser) test. The resin aliquot containing the linear epta-peptide was swollen for 2 hours in anhydrous DCM. After two hours, the vessel was heated to 45°C and a DCM solution of 2$^{nd}$ generation Grubbs catalyst (0.5 mole equiv. calculated on the basis of 0.5 mmol/g of peptide) was added[124,125]. The suspension was then stirred for 48 h at 45 °C. The resin aliquot was washed with DCM, DMF, and MeOH, then swelled for 45 min at room temperature in DMF[126,127]. Fmoc–Hag was deprotected (2.5 mL of 20% piperidine in DMF for 5 minutes, 4 time repeated) and coupled with Fmoc–D-Phe as described above, affording the on-resin cyclic octapeptide[128,129]. Activated DOTA(*tert*-Bu)$_3$ was added to the on resin-cyclic peptide affording the peptide-DOTA conjugate **1**, which was then deprotected and cleaved with TFA/$H_2O$/EDT/phenol (94:2:2:2, 3 h). The resin was filtered off, the solution was concentrated under reduced pressure and the peptide was precipitated by adding $Et_2O$. The collected solid was dissolved in water, lyophilized and re-dissolved in $H_2O$. The aqueous solution was pre-purified by SPE, eluting with an increased percentage of $CH_3CN$ in $H_2O$ (from 0% to 100%). The

fractions enriched of compound **1** were then subjected to the purification by semi-preparative RP-HPLC and characterized by ESI-MS. The MS spectrum of the pure compound showed a major peak of m/z $[M+2H]^{2+}$ ion and another small peak corresponding to $[M+H]^{+}$. The peptide-DOTA conjugate had a chromatographic purity > 97% (Table 1).

| **Compound number** | **Compound name** | **Mass Spectrum** | | **HPLC** | |
|---|---|---|---|---|---|
| | | **Calculated** | **Observed** | **$T_r$ (min)** | **Purity (%)** |
| 1 | DOTA-Peptide 1 | 1416,71 | 709.79 | 14.050 | 97 |

**Table 1:** Characteristic of DOTA-Peptide 1.

## 2 Determination of Somatostatin Receptor Affinity Profiles.

CHO-K1 and CCL39 cells stably expressing human SSTR1-5 receptors were grown, as described previously[109]. Cell membrane pellets were prepared and receptor autoradiography was done on 20 $\mu$m thick pellet sections (mounted on microscope slides), as described in detail previously[109]. For each of the tested compounds, complete displacement experiments were done with the universal SST radioligand [$^{125}$I]-[Leu$^{8}$,D-Trp$^{22}$,Tyr$^{25}$]-SST-28 using increasing concentrations of the unlabeled compounds ranging from 0.1 to 1000 nmol/L. SST-28 was run in parallel as control using the same increasing concentrations. $IC_{50}$ values were calculated after quantification of the data using a computer-assisted image processing system. Tissue

standards containing known amounts of isotopes, cross-calibrated to tissue-equivalent ligand concentrations, were used for quantification[109].

# 3 Studies performed with $^{177}$Lu-DOTA-Peptide 1.

## 3.1 Peptide radilabeling.

The radiolabelling procedure was optimized as follows: 10µg DOTA-Peptide-1 was diluted in 300µl ammonium acetate buffer (pH 5; 0,4M) and 1 mCi $^{177}LuCl_3$ was added for *in vitro* studies. It was increased the specific activity by adding 2.9 mCi $^{177}LuCl_3$ for serum stability assay and *in vivo* biodistribution studies. The solution was heated at 95°C for 30 minutes.

## 3.2 Quality control.

A quality control check was performed using analytic reversed phase high-performance liquid chromatography (RP-HPLC) with a radiometric detector, before adding 0.1% Human Serum Albumin, in 0.9% NaCl.

## 3.3 Serum Stability and Identification of Metabolites.

Serum stability test were performed on 1 ml fresh human serum, previously equilibrated in a 5% $CO_2$ (95% air) environment at 37°C, 100 µl of radiopeptide (corresponding to 30 pmol) were added. The mixture was incubated at 37°C, 5% $CO_2$ environment. At different time points, 100 µl aliquots were removed and treated with 200 µl EtOH. Samples were centrifuged for 5 minutes 1300 rpm to precipitate serum protein. The

supernatant was removed and collected to be checked by analytical HPLC and the pellets were washed twice with EtOH. The activity of the ethanolic phase and the precipitate were measured by a γ-counter. Both counts were compared to give the percentage of $^{177}$Lu complexes not bound to proteins or the percentage of radiometal transferred to serum proteins.

### 3.4 Cells line and culture conditions.

Human Embryonic Kidney (HEK-293) cell lines stably expressing T7-epitope tagged SSTR2 (HEK-SSTR2) were prepared as described before[130], and maintained by serial passage on monolayer in DMEM containing 10%FBS, L-glutamine, penicillin-streptomycin and 500g/ml G418 in a humidified 5% $CO_2$ atmosphere at 37°C.

The viability of the cells was assessed using trypan blue stain and counted under a microscope with a "Neubauer's counting chamber".

### 3.5 Radioligand Internalisation Studies.

For all cell experiments, 0.8–1.1 million HEK-SSTR2 cells were distributed in six-well plates pre-treated with poly-Lysine and incubated overnight at 37°C in a 5% $CO_2$/air atmosphere with internalization buffer (DMEM containing 1%FBS, L-glutamine, penicillin-streptomycin and 500g/ml G418) to obtain good cell adherence.

Further more, the internalisation rate was linearly corrected to 1 million cells per well in all cells experiments.

On the next day, the medium was removed, cells were washed twice with PBS and incubated for 1 h with fresh internalisation medium. Approximately 0.02 MBq per well of the $^{177/nat}$Lu-DOTA Peptide 1 (2.5 pmol per well) to a

final concentration of 1.67 nmol/l (corresponding to 500,000 cpm) were added to the medium and the cells were incubated at 37°C, 5% $CO_2$, with and without an excess of the DOTA Peptide 1 (1 μmol/l) to determine non-specific internalisation. At appropriate time periods (30 minutes, 1-2-4-24 hours), the internalisation was stopped by removing the medium and washing the cells with ice-cold PBS. To remove the receptor-bound radiopeptide, an acid wash was carried out with 0.1M glycine buffer pH 2.8 for 10 minutes on ice. This procedure was performed to distinguish between membrane-bound (acid-releasable) and internalised (acid-resistant) radioligand. Finally, the cells were solubilised with 1M aqueous NaOH and incubated for 10 min at 37° C. The culture medium, the receptor-bound and the internalised fractions were measured radiometrically in a γ-counter .

**3.6 Cellular Retention Studies.**

For cellular retention studies, HEK-SSTR2 cells stably transfected (about 1 million per well) were incubated with 2.5 pmol per well (1.67 nmol/l) of $^{177/nat}$Lu-labeled DOTA-Peptide 1 with and without an excess of the DOTA-Peptide 1 (1 μmol/l) for 120 minutes; then, the medium was removed and the wells were washed twice with 1 ml of ice-cold PBS. In each experiment, an acid wash for 5 minutes on ice with pH 2.8 glycine buffer was performed twice to remove the receptor-bound ligand. Cells were then incubated again at 37°C with fresh internalization buffer (DMEM containing 1% FBS, pH 7.4). After different time points, the external medium was removed for quantification of radioactivity in a γ-counter and replaced with fresh 37°C medium. Finally, the cells were solubilised in 1N NaOH and removed, and the internalized radioactivity was quantified in a γ-counter. The recycled fraction was expressed as the percentage of the total internalized amount per

1 million cells, and the internalization rate was linearly corrected to 1 million cells per well in all cell experiments.

### 3.7 Biodistribution studies in tumor bearing nude mice.

Animals were kept, treated and cared for in compliance with the guidelines of the Swiss regulations (approval #789).

Athymic female nude mice were implanted s.c. with about 10-12 million HEK-SSTR2 cells freshly suspended in sterile PBS. About seventeen days after the inoculation, mice showed solid palpable tumor masses (tumor weights: 60–150 mg), and were used for *in vivo* biodistribution experiments. Each animal was injected into the tail vein with 10 pmol $^{177/nat}$Lu-DOTA-Peptide 1 (0.15-0.2 MBq). To determine the non-specific uptake of radiolabelled peptide, a group of mice were injected with 20 nmol of DOTA-Peptide 1, 5 minutes before the injection of the radiopeptide.

The animals were sacrificed at 1, 4 and 24 hours after the injection of $^{177/nat}$Lu-DOTA-Peptide 1. The organs of interest were collected and weighed; their radioactivity was measured, and the %ID/g was calculated.

## 4 Studies performed with $^{111}$In-DOTA-Peptide 1.

### 4.1 Peptide radiolabeling.

10 µg DOTA-Peptide 1 was dissolved in 10 µL $dH_2O$, adding $CH_3COONH_4$ buffer 0.4M (pH 5) and $^{111}InCl_3$ was added, particularly 1 mCi for *in-vitro* assays and 2.9 mCi for *in-vivo* tests. The solution was heated at 95°C for 30 minutes, before adding human serum albumin.

## 4.2 Quality control.

Quality control was obtained using Sep-Pak C18 Cartridge. After the column preparation, 0.05-0.1 ml indium/$^{111}$In-DOTA-SST analog was pushed by a syringe into the Sep-Pak. After this passage, 5 ml of water were slowly pushed into the column and collected as "Fraction 1". Hydrophilic impurities are contained in this fraction. Similarly, 5 ml of methanol were pushed into the column, using a 5 ml syringe. This second fraction, that was collected as "Fraction 2" corresponds to the labeled peptide. The cartridge is also collected in a tube and counted, in fact all the not-elutable impurities remains into the column. The three tubes were counted in a gamma-counter and the radiolabeling purity was calculated as:

$$\%\ ^{111}\text{In-DOTA-SST analogue} = (\text{Fraction 2 activity/Total activity})$$

Where Total activity corresponds to the sum of Fraction 1, Fraction 2 and the activity remaining in Sep-Pak.

## 4.3 Cells line and culture conditions.

Rat pancreatic adenocarcinoma cell line (AR4-2J) stably expressing wild type rat-SSTR2 were maintained by serial passage on monolayer in DMEM containing 20% FCS and L-glutamine in a humidified 5% $CO_2$ atmosphere at 37°C.

The viability of the cells was assessed using trypan blue stain and counted under a microscope with a "Neubauer's counting chamber".

**4.4 Radioligand Internalisation Studies**.

Cells were seeded a density of 0.9 to 1.1 million per well in six-well plates and incubated overnight at 37°C in a 5% $CO_2$/air atmosphere in growth medium to obtain good cell adherence.
The loss of cells during the internalization experiments was <10%. Further more, the internalisation rate was linearly corrected to 1 million cells per well in all cells experiments.
This assay was performed maintaining the same condition previously described in the session 3.5, both for the radioligands concentration and time points.

**4.5 Cellular Retention Studies.**

For cellular retention studies, AR4-2J (about 1 million per well) were incubated with 2.5 pmol per well (1.67 nmol/l) of $^{111}$InDOTA-Peptide 1 with and without an excess of not radiolabeled peptide. The procedure adopted was the same described in 3.6 section.

**4.6 Biodistribution studies on balb-c mice.**

Groups of healthy balb-c mice were injected with 10 pmol $^{111}$In-DOTA-Peptide 1 and sacrificed at 1, 4, and 24 hours post injection. To evaluate the non-specific uptake of radiolabelled peptide, a group of mice were injected with 20 nmol of not radiolabeled DOTA-Peptide 1. The organs of interest were dissected, weighed, their radioactivity was measured by a gamma counter and the %ID/g was calculated.

# 5 Ligand Tracer®.

## 5.1 Cell culture and conditions.

A human papillary thyroid cancer cell line (NPA-87) was cultured and maintained by serial passage on monolayer at 37°C in RPMI 1640 supplemented with 10% FBS, sodium pyruvate, not essential amino acids, L-glutamine and penicillin/streptomycin, in a humidified incubator with 5% $CO_2$.

The viability of the cells was assessed using trypan blue stain and counted under a microscope with a "Neubauer's counting chamber".

## 5.2 Characterization of NPA-87.

NPA-87 cell line was characterized by Western Blot analysis and immunofluorescence studies for the determination of expression of all the five SSTRs subtypes.

### 5.2.1 Western Blot analysis.

Cells were maintained in a dish. When confluence was reached, cells were washed with ice-cold PBS and treated by ice-cold lysis buffer. After scraping adherent cells off the dish, the cells suspension were transferred into a pre-cooled microfuge tube, maintaining a constant agitation for 30 minutes at 4°C and centrifuged in a microcentrifuge at 4°C (20 minutes at 12,000 rpm). After discarding the pellet, Bradford assay was performed, using BSA as protein standard.

Sample of about 20-25 µg protein were used for western blot analysis. Sample were separated by electrophoresis on 10% SDS-polyacrylamide gel and transferred onto polyvinylidene difluoride membranes (BioRad). The membranes were probed with rabbit polyclonal antibodies anti SSTR1-5 (Santa Cruz Biotechnology) 1:1000 and horseradish peroxidase-conjugated anti-rabbit antibodies (1:2000; Santa Cruz) were used as secondary antibodies. The peroxidase reaction products were visualized by LumiGLO chemiluminescent substrate (Pierce Chemicals).

### 5.2.2 Immunofluorescence studies.

25,000-35,000 NPA-87 cell were seeded on chamber slide 8-well plates and incubated overnight at 37°C in a 5% $CO_2$/air atmosphere with the growth medium. On the next day, cells were washed twice by ice/cold PBS and pre-warm growth medium were added. Cells were re-equilibrated at 37°C in a 5% $CO_2$/air atmosphere.

Therefore, the cells were processed for immunofluorescence microscopy. After fixation and permeabilization for 7 minutes with ice-cold methanol (-20°C), cells were rinsed twice with PS (100mM PBS mixed with 0.15M sucrose), and blocked for 60 minutes at room temperature with PS containing 0.1% BSA. The cells were subsequently incubated for 60 minutes at room temperature with a rabbit polyclonal primary antibody anti SSTR1-5 (Santa Cruz Biotechnology) diluted 1:200 in PS containing containing 0.1% BSA and then washed three times for 5 min each with PS.

The cells were then incubated for 60 minutes at room temperature in the dark with the secondary antibody Alexa Fluor 488 goat anti-rabbit IgG (H+L) diluted in PS (1:150). Thereafter, the cells were washed three times for 5 minutes each with PS containing 0.1% BSA, embedded with mounting

media, and covered with a glass coverslip. The cells were imaged using a immunofluorescence microscope (Leica, Wetzlar, Germany) and a DP10 camera (Olympus, Tokyo, Japan).

## 5.3 Ligand Tracer®.

LigandTracer Instruments rely on a simple and robust technology for detecting protein-cell interactions in real-time. The key function is the possibility to detect interactions during incubation. This is made possible by including one active area (the seeded target cells) and one in situ reference area in the cell-dish. The cell-dish is then placed on a inclined, slowly rotating support. A solution containing a precise concentration of labeled protein is added to the dish and accumulates in the bottom part. Each revolution the cells will get in contact with the liquid. The detector is mounted over the upper part, collimated to read only the part of the dish that is essentially liquid-free.

When running, the activity is measured several times per revolution. If the protein binds to the cells, clear peaks will be seen in the graph. The peak height from each revolution is automatically extracted and can be followed over time (as in uptake/retention measurements). Alternatively, peak heights obtained from different concentrations of radiolabeled protein can be used to calculate the affinity of the interaction.
In particular, LigandTracer Yellow was adopted in this study. In fact, this instrumentation depicts how PET/SPECT markers bind to cells. The instrument preparation can be made well in advance of the actual measurement, which allows for unmet time-efficiency when working with rapidly decaying nuclides.

Ligand Tracer Yellow is mainly used for uptake/retention measurements, which reveals the kinetics of the PET/SPECT-marker interaction with cells.

### 5.4 Affinity assays with Ligand Tracer® and pharmacological studies.

NPA-87 cells were seeded (about 1,000,000 per dish) in a local part of a poly-Lysine pre-treated cell dish (diameter= 89 mm), as indicated in Figure 1.

The seeded cells were allowed to attach firmly to the dish surface for 24 hours maintaining inclined the dish at 37°C in a humidified incubator with 5% $CO_2$.

The dish was then placed on an inclined, rotating support where a radiation detector was mounted over the elevated part. Cell culture medium containing a low concentration (0.1 nM) of $^{111}$In-DOTA Peptide 1 or OctreoScan® were added to the dish and the detector registered the intensity as a function of rotational position. Every about 20 minutes, the concentration was increased by addition of a small amount of radioligand stock solution to the medium already present in the dish. During the last incubation, it was obtained a concentration of 550 nM on the culture medium. The procedure was repeated until a sufficiently high concentration had been reached. No washes of the cell dish were performed throughout the affinity measurement. The affinity of the interaction was obtained by fitting an interaction model (monovalent binding) to the measured peak heights.

In a parallel experiments, NPA-87 cells were seeded (25,000 cells per well) on chamber slide 8-well plates and incubated overnight at 37°C in a 5% $CO_2$/air atmosphere with the growth medium. On the next day, cells were treated with 100 nM DOTA-Peptide 1 or DTPA-Octreotide at 37°C and 5% $CO_2$ in growth medium for 0, 30, 60 and 120 minutes.

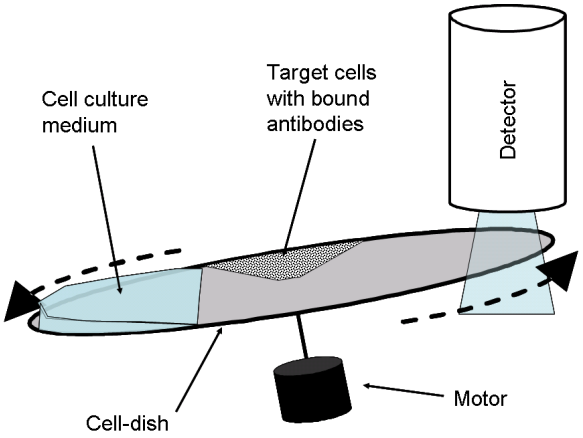


**Figure 1:** The principle of rotating RIA.

At the end of incubation times, incubations were stopped placing the chamber slide on ice. Therefore, the cells were processed for immunofluorescence microscopy. After fixation and permeabilization for 7 minutes with ice-cold methanol (-20°C), cells were rinsed twice with PBS, and blocked for 60 minutes at room temperature with PBS containing 1% BSA. The cells were subsequently incubated for 60 minutes at room temperature with an SSTR2a-specific primary antibody (SS-8000-RM BioTrend Chemikalien GmbH) diluted 1:500 in PS and then washed three times for 5 minutes each with PS containing 0.1% BSA.

The cells were then incubated for 60 minutes at room temperature in the dark with the secondary antibody Alexa Fluor 488 goat anti-rabbit IgG (H+L) diluted in PS (1:600). Thereafter, the cells were washed three times for 5 min each with PS containing 0.1% BSA, embedded with mounting media, and covered with a glass coverslip. The cells were imaged using a immunofluorescence microscope (Leica, Wetzlar, Germany) and a DP10 camera (Olympus, Tokyo, Japan).

# 6 Pharmacological studies.

## 6.1 Immunofluorescence studies: SSTR2 internalisation.

25,000-35,000 AR4-2J cell line expressing native wild type SSTR2 were seeded on chamber slide 8-well plates and incubated overnight at 37°C in a 5% $CO_2$/air atmosphere with the growth medium. On the next day, cells were washed twice by ice/cold PBS and pre-warm growth medium were added. Cells were re-equilibrated at 37°C in a 5% $CO_2$/air atmosphere.

One hour later, cells were treated with 100 nM DOTA-Peptide 1 at 37°C and 5% $CO_2$ in growth medium for 0, 5, 15, 30 minutes. Additionally, in parallel experiments, cells treated with 100 nM DOTA Peptide 1 for 30 minutes at 37°C and 5% $CO_2$ and were subsequently washed with PBS and incubated for 30 minutes in an agonist-free medium at 37°C and 5% $CO_2$. At the end of incubation times, incubations were stopped placing the chamber slide on ice. Therefore, the cells were processed for immunofluorescence microscopy. After fixation and permeabilization for 7 minutes with ice-cold methanol (-20°C), cells were rinsed twice with PS, and blocked for 60 minutes at room temperature with PS containing 0.1% BSA. The cells were subsequently incubated for 60 minutes at room temperature with an SSTR2a-specific primary antibody (SS-8000-RM BioTrend Chemikalien GmbH) diluted 1:500 in PS and then washed three times for 5 minutes each with PS containing 0.1% BSA.

The cells were then incubated for 60 minutes at room temperature in the dark with the secondary antibody Alexa Fluor 546 goat anti-rabbit IgG (H+L) diluted in PS (1:600). Thereafter, the cells were washed three times for 5 minutes each with PS containing 0.1% BSA, embedded with mounting

media, and covered with a glass coverslip. The cells were imaged using a immunofluorescence microscope (Leica, Wetzlar, Germany) and a DP10 camera (Olympus, Tokyo, Japan).

## 6.2 Immunofluorescence studies: investigation of intracellular localization of the internalized SSTR2.

To investigate the intracellular localization of the internalized SSTR2, it was examined its colocalization with the M6PR, a marker for the *trans*-Golgi network (TGN)/late endosomal compartment.

About 25,000-35,000 AR4-2J cells per well were seeded on chamber slide 8-well plates and incubated overnight at 37°C in a 5% $CO_2$/air atmosphere with the growth medium, cells were treated with or without 1 µM for 20 minutes at room temperature. Then the reaction was blocked and cells were fixed and permeabilized as described above.

The cells were subsequently incubated for 60 minutes at room temperature with the SSTR2a-specific antibody SS8000-RM (1:500 in PS) together with the monoclonal antibody to Mannose 6 Phosphate Receptor (cation independent)-late endosome marker (M6PR abcam ab 2733) (5 µg/ml in PS). The cells were washed and then incubated sequentially with Alexa Fluor 546 goat anti-rabbit IgG (H+L) diluted in PS (1:600) and then, after further washing, with the Alexa Fluor 488 goat antimouse IgG (H+L) diluted in PS (1:400), each for 60 minutes at room temperature in the dark.

Thereafter, the cells were washed three times for 5 minutes each with PS containing 0.1% BSA, embedded with mounting media, and covered with a glass coverslip.

The cells were imaged using a immunofluorescence microscope (Leica, Wetzlar, Germany) and a DP10 camera (Olympus, Tokyo, Japan).

# 7 Investigation of the activation of the apoptotic pathway.

## 7.1 TUNEL assay.

Apoptotic cells were visualized by direct fluorescence fragment end labelling of DNA breaks (TUNEL) using a commercially available kit (Fluorescein-FragEL; Calbiochem).

About 150,000 AR4-2J cells expressing native wild type SSTR2 were seeded on chamber slide 4-well plates and incubated overnight at 37°C in a 5% $CO_2$/air atmosphere with the growth medium. On the next day, cells were washed twice by ice/cold PBS and pre-warm growth medium were added. Cells were re-equilibrated at 37°C in a 5% $CO_2$/air atmosphere.

One hour later, cells were treated with different concentrations of DOTA-Peptide 1 (from 0.1nM to 1000nM) at 37°C and 5% $CO_2$ in growth medium. Incubations were stopped 16-18 hours after, placing the chamber slides on ice. Cells were washed twice by PBS, then cells were fixed in 4% formaldehyde (in 1X PBS) for 15 minutes at room temperature. After this passage, cells were washed twice with PBS and permeabilized with proteinase K (1:100 in 10 mM Tris HCl buffer, pH 8) for 20 minutes at room temperature. Subsequently, a 30 minutes of incubation TdT Equilibration buffer (1:5 with $dH_2O$ CalbioChem) at room temperature was performed. The next passage corresponds to the labelling reaction. The cells were incubated with the TdT Labelling Reaction mixture composed by Fluorescein-FragEL™ TdT labelling reaction mix and TdT enzyme. Cells were covered with 60 µl of the mixture and incubated in a humidified chamber at 37°C for 90 minutes. To visualise the entire cellular population on Sytox® Orange Nucleic Acid Stain (0.1 µM Molecular Probes) were incubated at room temperature for 10 minutes.

Thereafter, the cells were washed three times with PBS, embedded with mounting media, and covered with a glass coverslip. The cells were imaged using a immunofluorescence microscope (Leica, Wetzlar, Germany) and a DP10 camera (Olympus, Tokyo, Japan).

# RESULTS

## 1 Peptide synthesis.

In the method here reported it was used the H–L-Thr(*t*Bu)–ol–2-chlorotrityl resin (0.5 mmol/g) which already contains the C-terminal [Thr(ol)$^{15}$]. The elongation of the peptide sequence was stopped after the coupling of Hag$^{3}$ residue, with the aim of removing any possible interference of the aromatic ring of the N-terminal D-Phe$^{2}$ on the correct orientation of the allylglycine side chains required by the next ring-closing reaction. The linear hepta-peptide was then converted by RCM with a 2$^{nd}$ generation Grubbs catalyst to the corresponding cyclic analogue[124,125,126,127].

The D-Phe$^{2}$ terminal residue was added only after the cyclization step[128,11] The last step was the coupling of the prochelator DOTA (*tert*-Bu)$_3$ to the N-terminus of the peptide, affording compound **1**. Cleavage of the fully protected conjugates from the resin was obtained by the cleavage mixture TFA/$H_2O$/EDT/phenol (94:2:2:2, 3 h) which afforded also the free carboxylic groups of the DOTA moiety.

## 2 Determination of Somatostatin Receptor Affinity Profiles: Binding Affinity to SSTR1–5 Receptors.

All compounds were tested for their ability to bind to the five human SST receptor subtypes in complete displacement experiments using the universal SST radioligand [$^{125}$I]-[Leu$^{8}$,D-Trp$^{22}$,Tyr$^{25}$]-SST-28. SRIF-28 was run in parallel as control. $IC_{50}$ values were calculated after quantification of the data using a computer assisted image processing system. The data are shown in **Table 1**.

| Peptide | hSSTR1 | hSSTR2 | hSSTR3 | hSSTR4 | hSSTR5 |
|---|---|---|---|---|---|
| **Peptide 1** | **>1000** | **9.6±0,9** | **>1000** | **249±51** | **8.7±3.9** |
| **DOTA-Peptide1** | **>1000** | **8** | **>1000** | **>1000** | **100** |
| **SRIF-28** | **2.3±0.4**[131] | **3.0±0.2**[131] | **3.6±0.5**[131] | **1.6±0.3**[131] | **2.1±0.2**[131] |

**Table 1**: $IC_{50}$ (nM) values performed on membranes prepared from CHO-K1 cells stably expressing each human-SSTRs.

# 3 $^{177}$Lu-DOTA Peptide 1.

## 3.1 Peptide radiolabeling and Quality Control.

Quality control was performed by RT-HPLC with a radiodetector and demonstrated highly pure radioligands (98-100%).

## 3.2 Serum Stability and Identification of Metabolites.

The compound is stable in human serum. After 6 days few metabolites (<10%) were observed for this time period. No more than 10% of radioactivity was found in the protein fraction (pellet) at the first time points of the study (1, 2, 4 hours). A slide increase was observed up to 6 days when <15% of radioactivity was found in the protein fraction.

## 3.3 Radioligand Internalisation Studies.

The uptake of $^{177/nat}$Lu-DOTA-Peptide 1, evaluated on HEK-SSTR2 cells, demonstrated a time-dependent uptake in cells with a high specific internalization rate after 4 and 24 hours of incubation (**Graph 1** and **Table 2**). In particular, the internalised fraction of $^{177/nat}$Lu-DOTA-Peptide 1 after 4

and 24 hours incubation in HEK-SSTR2 corresponded to 38,63±3,26% and 57,68±3,00% respectively (2.5 pmol/$10^6$ cells). These experiments were done using $^{177}$Lu-DOTA-Tyr$^3$-octreotide as reference and it seemed that the two radiopharmaceuticals have similar behaviour.

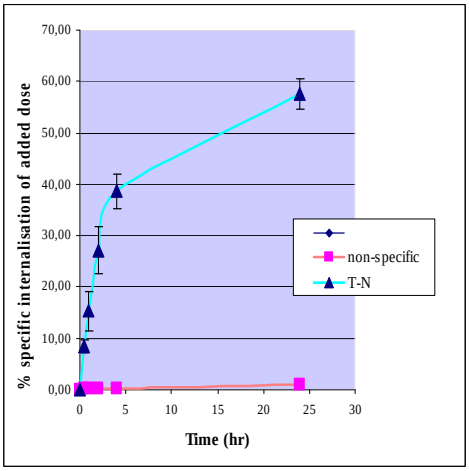


| Time (min) | Total | Non specific | Total-Non Specific |
|---|---|---|---|
| 0 | 0 | 0 | 0 |
| 30 | 8,49±1,24 | 0,17±0,03 | 8,33±1,25 |
| 60 | 15,52±3,83 | 0,21±0,02 | 15,32±3,84 |
| 120 | 27,41±4,48 | 0,26±0,04 | 27,16±4,50 |
| 240 | 38,95±3,28 | 0,32±0,04 | **38,63±3,26** |
| 1440 | 58,69±3,17 | 1,01±0,21 | **57,68±3,00** |

**Graph 1 and Table 2:** Radioligand internalisation studies were performed on HEK-293 cell line, stably expressing human SSTR2. Values and SD are the results of two independent experiments (each experiment was performed in triplicates).

### 3.4 Cellular Retention Studies.

In efflux studies, the radiopeptide was allowed to internalize for 120 minutes; the medium was removed and the cells were washed twice by cold PBS and two cold glycine buffer pH 2.8 washes were performed to remove the receptor-bound ligand. Warm medium was added (37° C) and after 15, 30, 60, 90, 240 minutes removed again, measured for radioactivity and replaced with a fresh one.

As shown in **Graph 2** and **Table 3** the externalization results showed time dependence: cells retained more than 50% of $^{177}$Lu-DOTA-Peptide 1 after four hours of incubation.

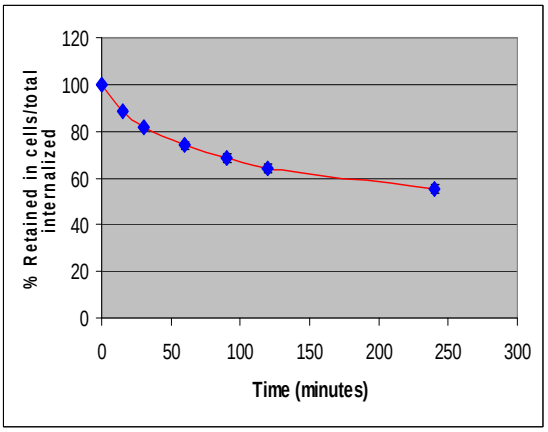


| Time points (min.) | % Retained in cells/total internalized |
|---|---|
| 0 | 100,00±0,00 |
| 15 | 88,47±0,44 |
| 30 | 81,42±0,78 |
| 60 | 73,9±1,46 |
| 90 | 68,63±1,74 |
| 120 | 63,89±1,97 |
| 240 | **55,40±2,07** |

**Graph 2- Table 3:** Efflux studies were performed on HEK-293 cell line, stably expressing human SSTR2. Values and SD are the results of two independent experiments (each experiment was performed in triplicates).

### 3.5 *In vivo* biodistribution.

The pharmacokinetic studies were performed in nude mice bearing HEK-SSTR2 tumor animal model. The results are given in **Table 4** and **5** and in **Graph 3** as a percentage of injected dose per gram of tissue (%ID/g).

The biodistribution studies demonstrated, by the measurement of blood samples taken at each time point, that the radiolabelled peptide was cleared rapidly from the circulation. The highest tissue activity is in the kidney which can be explained by the renal excretion being the physiological way for the elimination of this radiopharmaceutical. The other organs demonstrated a very low uptake, except for the stomach and the pancreas, but it is well known that these organs express SSTRs[11,12 ,13 ,14]. At 24 hours time point more than 50% of the radiopharmaceutical was cleared from these organs.

A high radioligand accumulation was observed in the tumors at 1 and 4 hours post injection (22.69±5.36 and 23.69±1.74 %ID/g respectively).

| Organ | 1 h (hours) | 4 h | 4 h blocking | 24 h |
|---|---|---|---|---|
| Blood | 0,55±0,19 | 0,12± 0,02 | 0,10±0,01 | 0,04± 0,00 |
| Heart | 0,23± 0,09 | 0,08± 0,02 | 0,09±0,01 | 0,06± 0,01 |
| Liver | 0,80±0,16 | 0,68±0,06 | 0,73± 0,06 | 0,46 ±0,00 |
| Spleen | 0,50 ±0,05 | 0,39± 0,05 | 0,28 ±0,05 | 0,34 ±0,05 |
| Lung | 0,91± 0,3 | 1,04±0,55 | 0,20 ±0,03 | 0,26 ±0,03 |
| Kidney | 10,63±2,03 | 11,16±1,19 | 9,85 ±0,91 | 6,69 ±0,7 |
| Stomach | 5,04±2,05 | 3,29 ±0,86 | 0,25±0,04 | 2,43± 0,12 |
| Intestine | 0,65±0,25 | 0,39 ±0,11 | 0,13 ±0,01 | 0,22± 0,03 |
| Adrenal | 0,44±0,19 | 0,59±0,26 | 0,38 ±0,21 | 0,52 ±0,21 |
| Pancreas | 2,87±0,61 | 1,85±0,32 | 0,16 ±0,02 | 0,95± 0,15 |
| Pituitary | 0,80±0,64 | 1,25±0,89 | 0,08 ±0,01 | 0,04 ±0,00 |
| Muscle | 0,11±0,04 | 0,05±0,02 | 0,05 ±0,00 | 0,03±0,02 |
| Bone | 0,71±0,09 | 0,65±0,2 | 0,22 ±0,08 | 0,66 ±0,07 |
| **Tumor** | **22,90±5,36** | **23,69±1,74** | **4,95 ±1,54** | **12,87±1,35** |

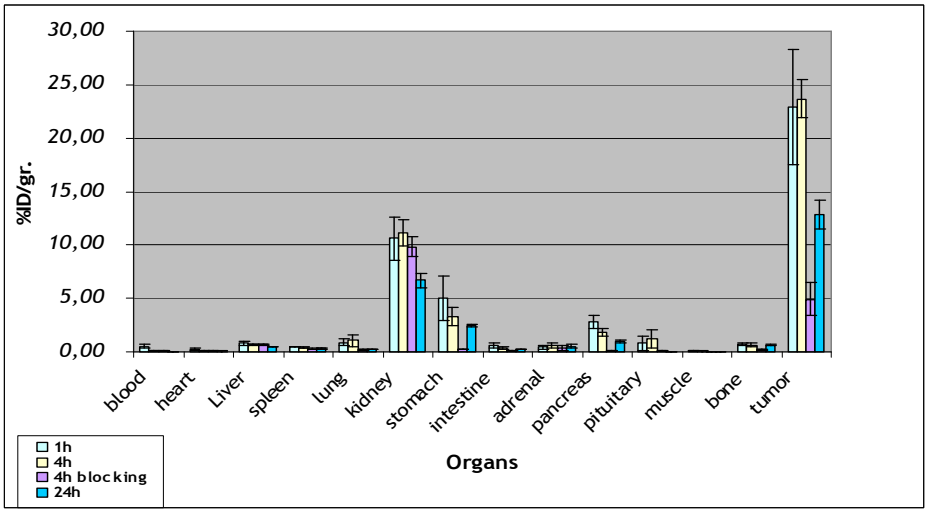


**Table 4 and Graph 3:** Biodistribution of $^{177}$Lu-DOTA Peptide 1 in a HEK-SSTR2 animal model (1, 4 and 24 hours post injection of the radiopharmaceutical).

| Ratio | 1h | 4h | 24 h |
|---|---|---|---|
| Tumor/kidney | 2.15 | 2.12 | 1.92 |
| Tumor/liver | 28.66 | 34.86 | 27.86 |
| Tumor/pancreas | 7.98 | 12.79 | 13.51 |
| Tumor/blood | 41.82 | 195.07 | 361.27 |
| Tumor/muscle | 212.42 | 521.38 | 377.49 |

**Table 5:** Tumor/normal tissue radioactivity ratios. Results are the mean of groups of 4 animals, except for the 4 hours blocking (n=3).

# 4 $^{111}$In-DOTA Peptide 1.

## 4.1 Peptide radiolabelling and quality control.

Radiolabelling yield demonstrated not successful results during the first phase of the study (55-76% of pure radiopeptide), but it was obtained 92% of pure radiopeptide during the last experiments.

## 4.2 Radioligand internalisation studies.

The uptake of $^{111}$In-DOTA-Peptide 1 was evaluated on AR4-2J cells and it was demonstrated a time-dependent uptake in cells with specific internalization rate after 4 hours of incubation (6,59%±0,92). The experiments were continued till 24 hour time point demonstrating high dose of internalised radioligand (27,23%±1,6) (**Graph 4**, **Table 6**). This experiments were performed using $^{111}$In-DOTA-Tyr$^3$-octreotide and $^{111}$In-DOTA-Tyr$^3$-octreotate as controls.

## 4.3 Cellular Retention Studies.

In efflux studies, the radiopeptide was allowed to internalize for 120 minutes; the medium was removed and the cells were washed twice by cold PBS and two cold glycine buffer pH 2.8 washes were performed to remove the receptor-bound ligand. Warm medium was added (37° C) and after 15, 30, 60, 90, 240 minutes removed again, measured for radioactivity and replaced with a fresh one. As shown in **Graph 5** and **Table 7** the externalization results showed time dependence: cells retained more than

50% of $^{111}$In-DOTA-Peptide1 after four hours of incubation, maintaining similar behaviour of $^{177}$Lu-DOTA-Peptide 1.

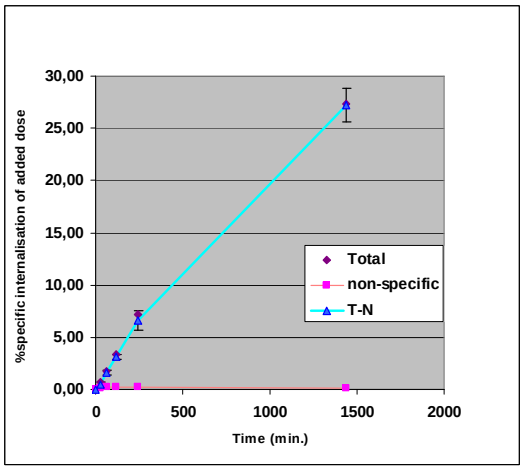


| Time (min) | Total | Non Specific | T-N |
|---|---|---|---|
| 0 | 0,00 | 0,00 | 0,00 |
| 30 | 0,75±0,11 | 0,1±0,14 | 0,50±0,16 |
| 60 | 1,70±0,24 | 0,2±0,09 | 1,61±0,27 |
| 120 | 3,35±0,26 | 0,23±0,1 | 3,16±0,23 |
| 240 | 7,16±0,77 | 0,22±0,56 | **6,59±0,92** |
| 1440 | 27,31±1,61 | 0,09±0,01 | **27,23±1,6** |

**Graph 4, Table 6: :** Radioligand internalisation studies were performed on AR4-2J cell line, stably expressing SSTR2. Values and SD are the results of three independent experiments (each experiment was performed in triplicates).

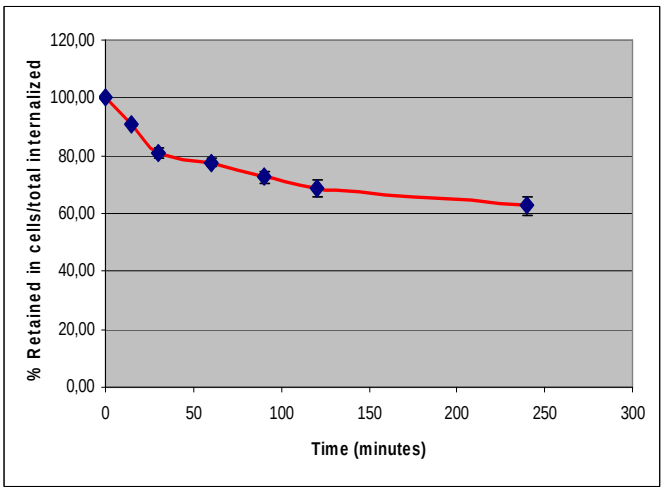


| Time points (min.) | %Retained in cells/total internalized |
|---|---|
| 0 | 0,00 |
| 15 | 90,67±0,32 |
| 30 | 80,80±1,81 |
| 60 | 77,76±1,56 |
| 90 | 68,63±1,74 |
| 120 | 68,56±2,89 |
| 240 | **62,75±3,04** |

**Graph 5, Table 7**: Efflux studies were performed on AR4-2J cell line, stably expressing native SSTR2. Values and SD are the results of three independent experiments (each experiment was performed in triplicates).

## 4.4 *In vivo* biodistribution.

Pharmacokinetic studies were performed in balb-c healthy mice. Results (%ID/g) showed high radioligand accumulation in the pituitary gland at 1, 4 and 24 hours post injection, but the stomach and the pancreas demonstrated a good uptake of the radiopharmaceutical too. These results are compatible with normal SSTRs expression with exception of the kidneys that demonstrated not specific uptake, because of the radiopharmaceutical clearance. The other organs demonstrated a low uptake. At the 24 hours time point a good clearance was observed for all tissues, the only exception are constituted by kidneys and pituitary gland, where the uptake remained high (**Graph 6**, **Table 8**).

| Organs | 1h | 4h | 4h blocking | 24 h |
|---|---|---|---|---|
| blood | 0,95±7,8E-05 | 0,67±0,0014 | 0,10±0,0008 | 0,18±0,0009 |
| heart | 0,42±0,0003 | 0,29±0,0002 | 0,08±0,0005 | 0,10±2,830E-05 |
| Liver | 0,82±0,0008 | 0,76±0,0015 | 0,52±0,0032 | 0,44±0,0003 |
| spleen | 0,51±0,0010 | 0,41±0,0005 | 0,15±0,0010 | 0,28±5,201E-05 |
| lung | 1,87±0,0005 | 1,48±0,0035 | 0,27±0,0022 | 0,49±0,0017 |
| kidney | 13,39±0,0011 | 13,57±0,0057 | 7,15±0,0596 | 4,88±0,0009 |
| stomach | 1,13±0,0032 | 1,04±0,0025 | 0,29±0,0016 | 0,46±0,0011 |
| intestine | 0,43±0,0026 | 0,44±0,0008 | 0,22±0,0016 | 0,17±0,0004 |
| adrenal | 0,33±0,0117 | 0,15±0,0003 | 0,02±4,75E-05 | 0,18±0,0001 |
| pancreas | 0,57±0,0022 | 0,43±0,0021 | 0,17±0,0010 | 0,27±0,0001 |
| pituitary | 14,93±0,008 | 7,45±0,0024 | 7,99±0,080 | 8,10±0,0070 |
| muscle | 0,26±0,0015 | 0,20±0,0006 | 0,10±0,0007 | 0,15±0,0003 |
| bone | 0,75±0,0006 | 0,54±0,0023 | 0,16±0,001 | 0,27±0,0012 |

**Table 8:** Biodistribution of $^{111}$In-DOTA Peptide 1 in healthy balb-c mice (1, 4 and 24 hours post injection of the radiopharmaceutical).

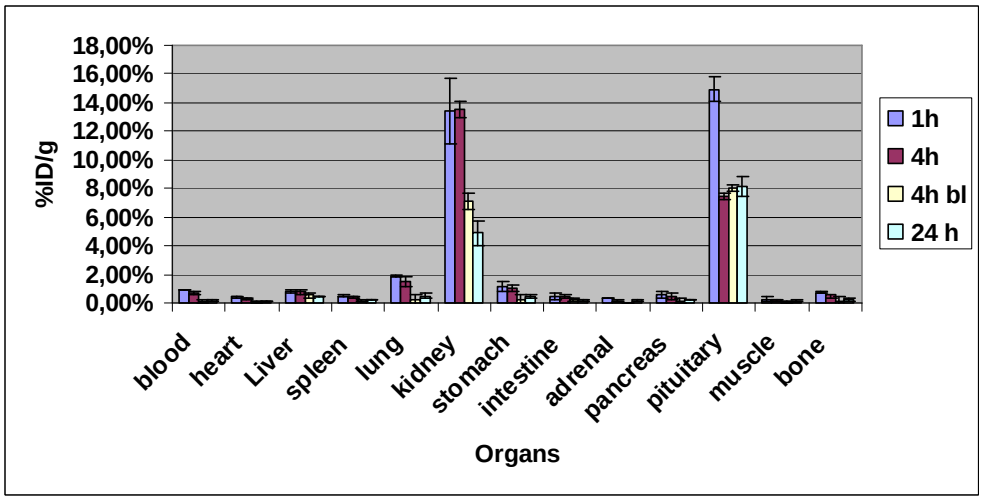


**Graph 6:** Biodistribution of $^{111}$In-DOTA Peptide 1 in healthy balb-c mice (1, 4 and 24 hours post injection of the radiopharmaceutical).

# 5 Ligand Tracer®.

## 5.1 Characterization of NPA-87.

### 5.1.1 Western Blot analysis.

Western Blot evidenced the presence of SSTR-2 expression in NPA-87 cell line with a concomitant presence of other SSTRs subtypes, particularly, it was demonstrated the expression of SSTR3 and SSTR5 (**Picture 1**).

### 5.1.2 Immunofluorescence studies.

Immunofluorescence studies confirmed the results obtained by Western Blot analysis. Even in this case it was observed a positivity for the expression of SSTR2, SSTR3 and SSTR5 (**Picture 2**).

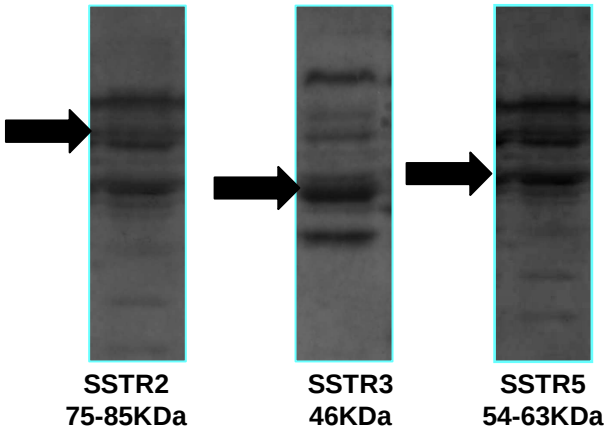


**Picture 1:** SSTR2-3-5 expression on NPA-87 cell line by Western Blot Analysis.

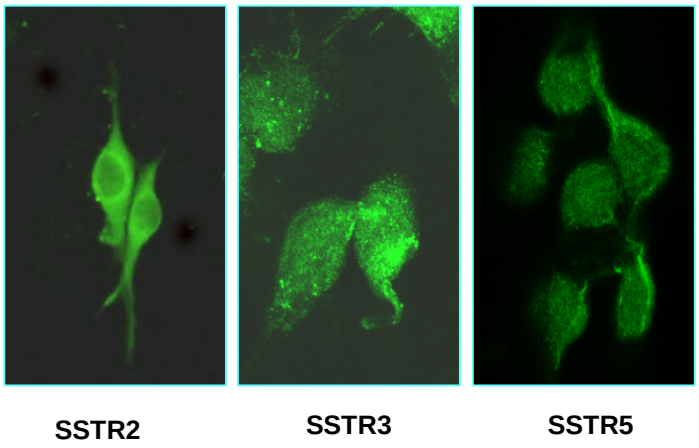


**Picture 2:** SSTR2-3-5 expression on NPA-87 cell line by Immunofluorescence studies.

## 5.2 Affinity assays with Ligand Tracer® and pharmacological studies.

Radiolabeling and quality control of $^{111}$In-DOTA-Peptide 1 were performed as previously described and the same results were obtained.

OctreoScan® and $^{111}$In-DOTA-Peptide 1 affinity were measured with LigandTracer® on NPA87 cells. In parallel, pharmacological studies were performed, demonstrating a precise different intracellular localization of SSTR2 after the treatment with the cold peptides at each time point of the study.

DTPA-Octreotide and the DOTA-Peptide 1 have generated similar answer if compared to the affinity results obtained with LigandTracer® experiments with the same radiolabeled peptides. Preliminary results of the affinity studies with LigandTracer® on NPA-87 are reported in **Graph 7** both for OctreoScan® and $^{111}$InDOTA-Peptide 1, where $B_{max}$ and $K_D$ are reported. $^{111}$InDOTA-Peptide 1 has similar pharmacological proprieties as OctreoScan® on cell lines and these results suggest that after radiolabelling the peptide retain affinity and uptake in selected cell lines.

Pharmacological assays by immunofluorescence demonstrated that there is a precise localisation of the ligand-receptor complex at different time points (**Picture 3**) and it seems that the process ends after two hours of incubations.

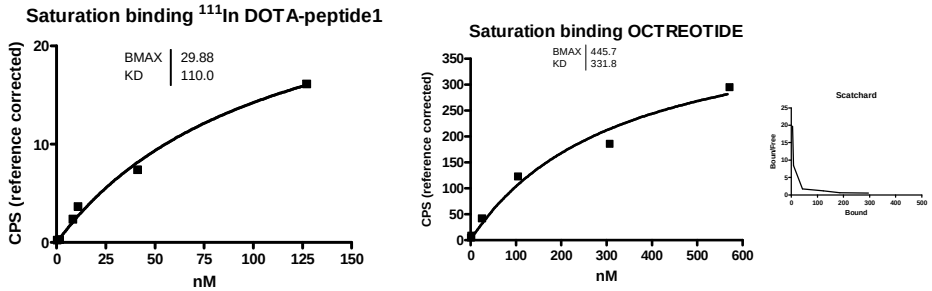


**Graph 7:** Saturation binding with $^{111}$InDOTA-Peptide 1 and Octreoscan® on NPA-87 cell lines.

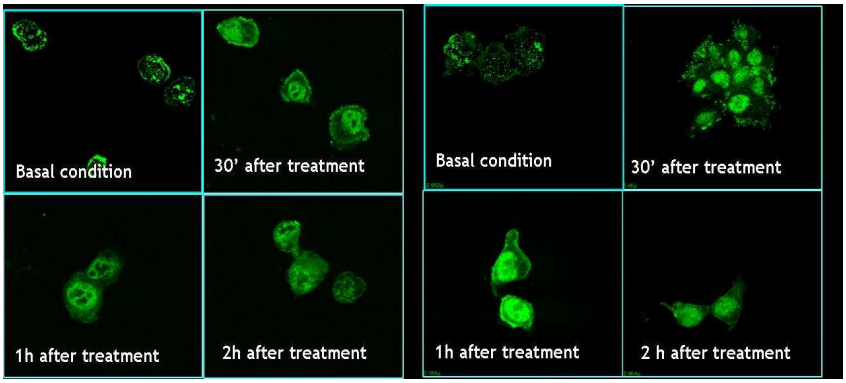


**Picture 3:** Sequential intracellular localization of SSTR2 after treatment with cold peptides. DTPA-Octereotide (on the left) and DOTA-Peptide 1 (on the right) have generated similar response.

# 6 Pharmacological studies.

## 6.1 Immunofluorescence studies: SSTR2 internalisation.

The internalization assay was validated through a series of experiments in AR4-2J cells showing that SSTR-2 is membrane bound in the absence of agonist; that there is a time, temperature, and agonist concentration dependency for SSTR2 internalization (**Picture 4 A-E**).

**Picture 4B** illustrates that an early phase of agonist-induced SSTR2 internalization is noticed *in vitro* at 5 minutes, as shown by the monitoring of SSTR2 trafficking with immunofluorescence microscopy. Furthermore, this *in vitro* SSTR2 internalization is also rapidly completed within minutes, as seen in the 15- and 30-minutes times (**Picture 4C** and **4D**). Finally, when the agonist is removed from the medium (washing step), the SSTR2 receptors are relocated to the cell surface as soon as 30 minutes after washing (**Picture 4E**).

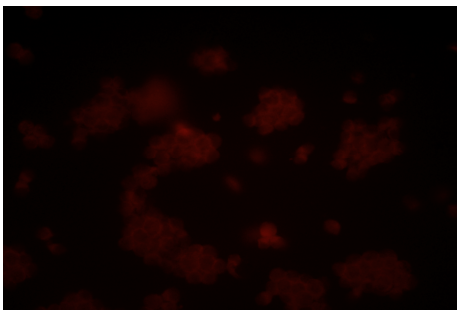

**A**

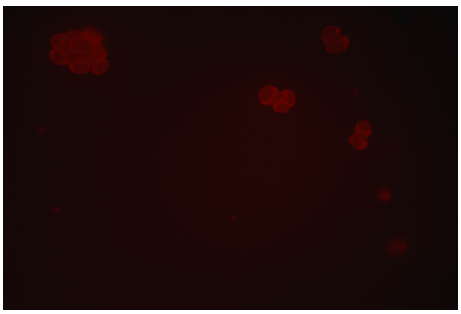

**B**

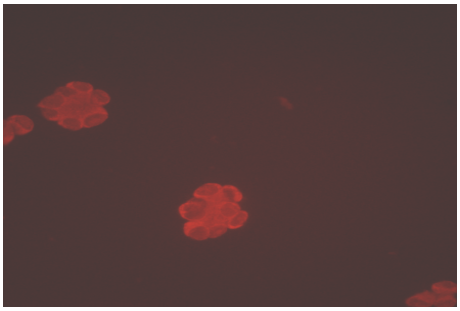

**C**

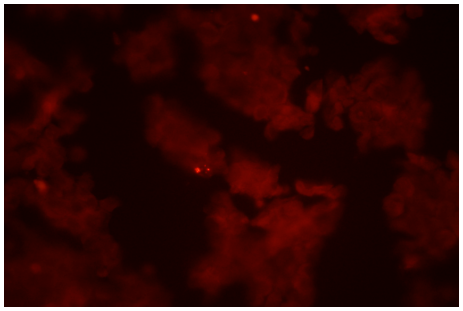

**D**

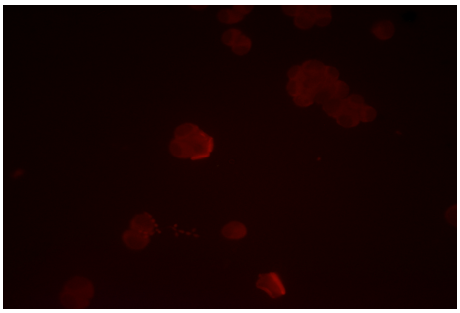

**E**

**Picture 4 A-E:** Agonist-induced internalization of SSTR2 receptor in AR4-2J. AR4-2J were treated either with vehicle alone (A) or with 100 nM DOTA- Peptide 1 for 5 (B), 15 (C), or 30 min (D) at 37°C and 5% $CO_2$. Moreover, in parallel experiments, cells treated with 100 nM DOTA-Pepide 1 for 30 min at 37° C and 5% $CO_2$ were subsequently washed with PBS and then incubated for 30 min in agonist-free medium at 37° C and 5% $CO_2$ (E). Cells were then fixed, permeabilized, labeled with SSTR2 primary antibody, and processed for immunofluorescence. Internalization is already observed at 5 min and is completed at 30 min. After subsequent washing and incubation in agonist-free medium, SSTR2 receptors are back at plasma membrane.

## 6.2 Immunofluorescence studies: investigation of intracellular localization of the internalized SSTR2.

In this session, it was demonstrated that SSTR2 is internalized via clathrin-coated vesicles and localizes to mannose 6-phosphate receptor–positive (M6PR) intracellular compartments, most likely the trans-Golgi network (TGN)/late endosome.

In **Picture 5**, it was allowed to observe the 1 µM internalisation of SST analogue after an incubation of 20 minutes at room temperature. SSTR2 and

M6PR are not completely overlapping, but it was demonstrated SSTR2 is internalized via clathrin-coated vesicles.

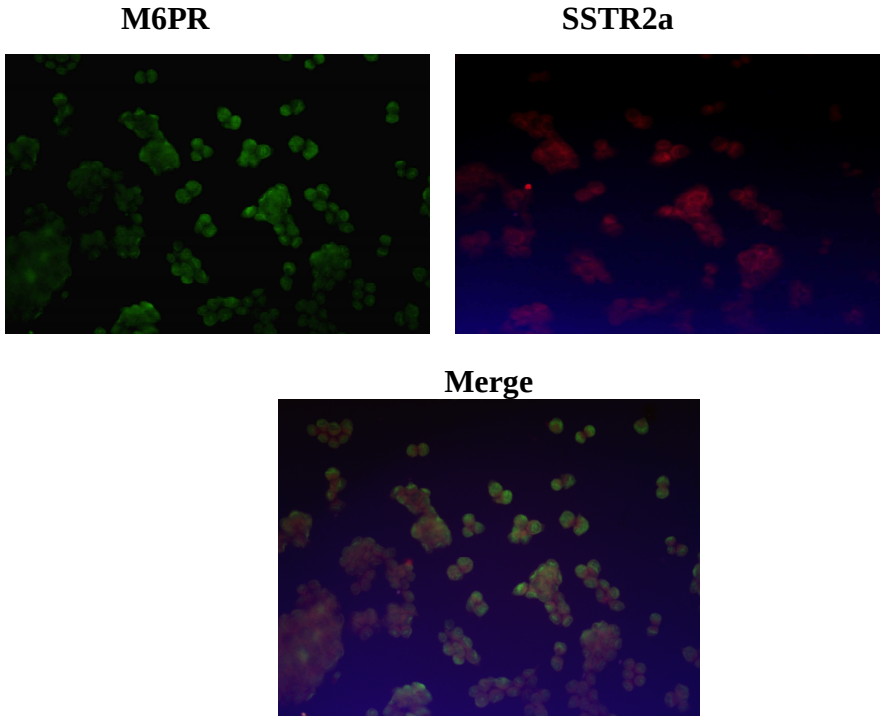


**Picture 5:** Agonist-induced internalization of SSTR2 in AR4-2J. AR4-2J were treated with 1 µM DOTA- Peptide 1 for 20 min at room temperature. SSTR2 is internalized via clathrin-coated vesicles and localizes to mannose 6-phosphate receptor–positive (M6PR) intracellular compartments, most likely the trans-Golgi network (TGN)/late endosome. Merge corresponds to the M6PR and SSTR2 pictures overlapping.

# 7 Investigation of the activation of the apoptotic pathway.

## 7.1 TUNEL assay.

TUNEL assay did not demonstrate any positivity. Cells obiuvesly appered stressed and probably the pharamcological treatment with an high dose of SST analogues induced a cytostatic effect on cells. This experiment was

performed using DOTA-Tyr$^3$-octreotide as control, that demonstrated to have the same behaviour of DOTA-Peptide 1.

This are only a preliminary results, most probably other cellular pathways are involved, particularly the actention have to be focus on cytostatic effect due to the activation of SSTR2 by a SST analogue. It seems that apoptosis is not the predominantly activated pathway by SSTR2, for this reason this experimental session has to be considered only a first step of another important session that have to be studied in further experimental protocols.

# DISCUSSION

The importance of peptides probes in diagnosis and therapy is growing up in the last decade. Receptors, and in particular GPCRs, are expressed with high density in tumoral cells. For this reason, in recent times, regulatory peptides receptors became an interesting and important target in cancer imaging and treatment. This is possible, because cellular membrane receptors (GPCRs) have the peculiarity to be overexpressed in tumoral cells, while their density is quite low in physiologic healthy organs, avoiding a general toxicity.

SSTRs represented the first example of peptide-based probe for cancer imaging and for PRRT, since these receptors are over-expressed on most neuroendocrine tumors, GEP and other cancers such as bronchial NET, breast cancer, RCC and some lymphomas. In more recent times, other receptors have been used as targets for cancer imaging by regulatory peptides. This is the case of cholecystochkinin/gastrin and GLP-1[132] analogues for NETs, bombesin[133] and neuropeptide Y[134] analogues for prostate and breast cancers, Arg-Gly-Asp peptides for neoangiogenesis[135]. Even if all these analogues are still in preclinical or early stage clinical development, some of them seem very promising.

Specific target of tumors through selective molecules, either for diagnostic or therapeutic reasons, are promising in oncology, compared with earlier less specific approaches. In fact, peptides demonstrated some features that make them very attractive and advantageous compared to the other molecules used in clinic. For example, full molecules antibodies presents some problems due to poor diffusion and target accessibility, while peptides have small size

(<10,000 Da), good tissue diffusion and target accessibility, but also no antigenicity, easy synthesis and easy adequate radiolabelling.

The action of these peptides depend, first of all, on affinity for specific cell membrane surface receptors that, once bound to these ligands, transfer them to within the cell (peptide-receptor internalization) and eventually to the perinuclear and nuclear location, where they persist for relatively long periods. Hence, hypothetically once firmly labelled, the radioligand is thereby useful for imaging and therapy[136].

Therefore, principle of peptide-based cancer imaging presumes that an analogue, linked to a chelator that allows a stable radiolabeling with different radiometals ($^{111}$In, $^{68}$Ga and $^{99m}$Tc) for *in vivo* imaging is injected to the patient intravenously. The radiopharmaceutical will distribute through the body. In case of the high expression of the specific receptor on tumoral cells, the radiopeptide will bind to them and a subsequently internalisation of the radiolabeled peptide-receptor complex will occur. This process will allow to γ-camera ($^{111}$In and $^{99m}$Tc- SST analogues) or PET scans ($^{68}$Ga SST analogues) to underline the high specific uptake of the tumoral masses compared with the other organs, that demonstrate a low or none accumulation of radioactivity. Kidneys or liver are the other organs that will record a consistent accumulation of radioactivity. This is due to the physiological excretion of the radiopharmaceutical. SST analogues demonstrated a predominantly renal excretion, with the exception of the first radiolabeled SST-analogue further abandoned in clinic, the very high lipophilic $^{123}$I-[3-iodo-Tyr$^3$]-octreotide, characterized by high accumulation in liver, thus perform poorly when imaging abdominal area.

The gold standard for *in vivo* imaging of SSTR2 expressing tumors is now represented by OctreoScan® ($^{111}$In-DTPA-octreotide). In this case, excretion

pathway is predominantly by kidneys, but it can be observed an epatobiliary excretion of low entity, giving sometimes a not fully clear abdomen imaging. Common indications for OctreoScan® scintigraphy include the detection and localization of a variety of NET, other tumors and their metastases, the staging of patients with neuroendocrine tumors, the follow-up of patients with known disease, and lastly the selection of patients with inoperable and/or metastatic tumors for PRRT.

Subsequently, new analogues were studied. In particular, the new peptides have maintained octreotide as skeleton, introducing some modifications, as aminoacidic substitutions or the introduction of a synthetic aminoacids. The choice of adopting DOTA (1,4,7,10-tetraazacyclododecane-1,4,7,10-tetraacetic acid) as chelator brought some advantages compared to DTPA. DOTA forms a kinetically and thermodynamically stable metal complexes, because the radiometal is encapsulated and embedded in the DOTA-skeleton, where it is protected by the attack of competing ligand present in human tissue and body fluids.

Limit of DOTA-SST analogues is their hydrophylicity, resulting in a predominantly renal excretion and a potentially kidney damage. It is important to avoid kidneys injure, especially for those patients where PRRT is required. This inconvenience is now gets over adopting two strategies: kidneys protection by ramified amino acids infusions in patients and introduction of some modifications in the octapeptide amino acidic sequence, improving in lipophilicity and maintaining the affinity profiles previously obtained.

$^{90}$Y and $^{177}$Lu radiolabeled SST-analogues, particularly DOTA-Tyr$^3$-octreotide and DOTA-Tyr$^3$-octreotate, are currently adopted for PRRT in different clinical setting among the word. This two radiopharmaceuticals have an important background and important preclinical and clinical studies

are performed until now. Most consistent clinical studies have been performed in the nuclear medicine centre at the IEO (Milan, Italy) and in Rotterdam. Paganelli et al. published that partial and complete remissions were obtained in 28% of 87 patients with neuroendocrine tumors[137] treated by $^{90}$Y-DOTA-Tyr$^3$-octreotide. A multicenter phase-1 study performed in Rotterdam (The Netherlands), Brussels (Belgium), and Tampa (USA) with $^{90}$Y-DOTA-Tyr$^3$-octreotide demonstrated in 58 patients received escalating doses up to 400 mCi (14.8 GBq)/m$^2$ in four cycles or up to 250 mCi (9.3 GBq)/m$^2$ single dose, no maximum tolerated single dose[138]. The cumulative radiation dose to kidneys was limited to 27 Gy. All received ramified aminoacids concomitant with $^{90}$Y-DOTA$^0$,Tyr$^3$-octreotide for kidney protection. Three patients had dose-limiting toxicity: one had liver toxicity, one had thrombocytopenia grade 4, and one had MDS[138].

DOTA-Tyr$^3$-octreotate has demonstrated very successful results in preclinical studies, in particular in terms of tumor regression and animal survival in a rat model[139]. The affinity results performed by Reubi *et al*. and published in 2000[24], demonstrated a nine fold increase in affinity for the SSTR subtype 2 for DOTA-Tyr$^3$-octreotate if compared with DOTA-Tyr$^3$-octreotide, and a six- to sevenfold increase in affinity for their Yttrium-loaded counterparts, and clinical studies performed in patients with large NET demonstrated that DOTA-Tyr$^3$-octreotate gave a partial tumor remission of 35% and complete remission in 3%[140].

$^{177}$Lu-DOTA-Tyr$^3$-octreotate allow to obtain a higher absorbed doses in most of the tumors with about equal doses to potentially dose-limiting organs. Because of the lower tissue penetration range of $^{177}$Lu if compared with $^{90}$Y, it may be especially important for small tumors. Moreover, if it are compared the residence time in tumors for $^{177}$Lu-DOTA-Tyr$^3$-octreotide and $^{177}$Lu DOTA-Tyr$^3$-octreotate in the same patients in a therapeutical setting,

we found a factor 2.1 in favour of $^{177}$Lu-DOTA-Tyr$^{3}$-octreotate[141]; and at the moment, $^{177}$Lu-DOTA-Tyr$^{3}$-octreotate seems to be the radiolabeled SST-analog of choice when performing PRRT.

In more recent studies, new SST-analogs with a broader receptor subtype affinity profile has been initiated. These new compounds, DOTA-NOC and DOTA-BOC, present a substitution in position number 3 of the peptide, where Tyrosine are replaced by synthetic alanines: 1-naftil-alanine (DOTA-NOC) or a benzothienyl-alanine (DOTA-BOC) and demonstrated high affinity for hSSTR2-5[142] and DOTA-NOC for SSTR-3 too[142].

This two radiopeptides are now in clinical phase for scintigrafic acquisition, but their availability is difficult, because are not on the trade, consequently their utilise is limited to a small numbers of diagnostic centres.

Studies performed by $^{68}$Ga-DOTANOC demonstrated a very successful imaging for the detection of small tumor lesions, especially for lymph nodes and bones which is attributable to the high target to not-target ratios obtained to this SST-analogue with a broader receptor subtypes affinity profiles[143]. For the peculiarities of this radiopeptide, DOTA-NOC seems a good candidate for PRRT.

At moment, clinical protocols foresee that malignant cells of tumoral masses are highlighted with $^{111}$In-DTPA-octreotide (OctreoScan®) enables *in vivo* imaging tumors and metastasis[144,145]. Thanks to the develop of $^{68}$Ge/$^{68}$Ga generators and PET-CT scans, a more accurate imaging of tumors is now obtained by the use of $^{68}$Ga-DOTA-SST analogues. A study performed in a small group of patients by Gabriel M. *et al*[146] demonstrated that $^{68}$Ga-DOTA-Tyr$^{3}$-octreotide performed better results compared with conventional nuclear medicine examinations. In particular, the better imaging properties are based on the higherspatial resolution of PET and some beneficial pharmacokinetic

properties of $^{68}$Ga-DOTA-Tyr$^{3}$-octreotide. Anyway, $^{68}$Ga may not be used for dosimetric estimates.

The idea of this project derives from a precise clinic necessity, consisting in the research of new radiopharmaceuticals that can be adopted in the PRRT, in particular all those SSTRs expressing tumors that elude from any therapeutic plan. This is the case of thyroid cancers once they presented dedifferentiation. In fact, papillary e follicular thyroid cancers after the conventional treatment, develop locoregional recurrence (20%) and distant metastasis (10%), loosing the ability to uptake $^{131}$I and showing elevated serum tireogloguline (Tg) concentration[147]. Different studies have demonstrated that specific SST binding to membranes of normal thyroid tissues and thyroid carcinoma cell lines as well as disparate proliferative effects of different SST analogs on cell lines in monolayer cultures. To date, human carcinomas have been reported to express predominantly SSTR2, with limited expression of SSTR1, SSTR3, and SSTR4. SSTR5 expression in human cancers appears unique to thyroid cancer, except for a preliminary report of expression in human breast carcinomas. Various recent studies have described the visualization of metastases from follicular cell-derived thyroid carcinomas by means of somatostatin receptor scintigraphy although, in contrast to medullary thyroid carcinoma, these tumors are not of neuroendocrine origin. These findings are in agreement with the *in vitro* demonstration of specific somatostatin binding receptors in thyroid carcinoma cells. In the majority of these tumors, the expression of SSTR-1, SSTR-3, and SSTR-5 seems to predominate, and depending on the applied technique, in some tumors no SSTR-2 could be demonstrated at all. While the radiopharmaceutical specifically binds to the tumoral cells, the radiation emitted by the radionuclide can additionally exert a cytotoxic effect on

adjacent non-SSTR expressing cells, by cross-fire of the emitted particles diffusing within a certain range in tissues.

Generally, the current SST analogues in clinical use, octreotide and derivates, at clinically available doses, interacts with SSTR2 and some of them with SSTR5, but with a less affinity.

Because dedifferentiated thyroid cancers express SSTR3-5 with high density, while the SSTR2 expression seems to be very controversial, SST analogues with high affinity for SSTR3, SSTR5 or both are required.

In this study, a new SST analogue: DOTA-Peptide 1 was characterised.

The peculiarity of this SST analogue consists in the replacing of $Cys^2$-$Cys^7$ by two allyl-glycine linked together by a double bound. This avoids the problem of the disulphide bridge present in the others, that are subjected, once is injected throw the blood flow, to the attack of the endogenous reducing agents as glutathione oxidase or thioredoxin reductase, or of basic and nucleophilic agents. Another aminoacidic change that is important to underline is the presence of a 2-NaI in position 3 (pharmacophore).

The peptide was synthesized by solid phase synthesis giving a more than 95% of peptide purity.

Affinity profile were performed before and after DOTA coupling and it was demonstrated that the addition of DOTA is responsible of a loosing of affinity for hSSTR5.

DOTA-Peptide 1 does not showed an enthusiastic affinity profile results for hSSTR 2 (DOTA-Peptide 1 has an $IC_{50}$ of about 8 nM for hSSTR2, while DOTA-$Tyr^3$-octreotate $IC_{50}$ is 1,5±0,4 nM), but *in vitro* and *in vivo* experiments gave promising and important results.

In this project, internalisation rate, cellular retention and radio-binding proprieties of a new SST-analogue with a high affinity for SSTR2 was evaluated.

The first part of the study was performed in collaboration with the division of radiological chemistry, in the department of radiology of UHBS in Basel (Switzerland). DOTA-Peptide 1 was radiolabeled with $^{177}$Lu, a radiometal used for therapeutic purposes (β-emitter; 497 keV, 78%), but which also allows imaging (γ-emitter, 113 keV, 6%, 208 keV, 11%).

After the stability tests, demonstrating an high stability in human serum until 4 days, radioligand internalisation and cellular retention assays were performed on HEK-293 cell line stably expressing T7-epitope tagged human SSTR2 (HEK-SSTR2) and it was demonstrated that a very high radiopeptide accumulation in cells and a time-dependent internalisation. Particularly, it was observed that after 4 hours of incubation 38.63%±3.26 of radiopeptide is internalised. During these experiments a plateau was not reached, so incubations were continued till the 24$^{th}$ hour, where an high dose of internalised fraction was observed (57.68%±3.00). Internalisation assays were performed using $^{177}$Lu-DOTA-Tyr$^3$-octreotide as control, showing a similar behaviour between the two radiopeptides.

Cellular retention studies demonstrated that an high degree of radiopeptide is retained in cells after 4 hours of incubation (55.4% of radioactivity is retained in the cell from the total internalized conjugate). This is an important result because a prolonged intracellular retention is of importance if long-lived radionuclides are going to be used in therapy studies.

Finally, a very high tumor uptake resulted in tumor-bearing mouse model adopted in this part of the research project.

The biodistribution studies performed on female nude mice bearing HEK-SSTR2 tumors demonstrated, by the measurement of blood samples taken at each time point, that the radiolabelled peptide was cleared rapidly from the circulation (0.55±0.19 1 hour post injection; 0.12±0.02 4 hours post injection 0.04± 0.00 24 hours post injections). The highest tissue activity is in the

kidney (10.63±2.03 1 hour post injection, 11.16±1.19 4 hours post injection, 6.69 ±0.7 24 hours post injection) which can be explained by the renal excretion being the physiological way for the elimination of this radiopharmaceutical. The other organs demonstrated a very low uptake except for the stomach (5.04±2.05 1 hour post injection, 3.29 ±0.86 4 hours post injection and 2.43± 0.12 24 hours post injection) and the pancreas (2.87±0.61 1 hour post injection, 1.85±0.32 4 hours post injection, 0.95± 0.15 24 hours post injections), but it is well known that these organs express SSTRs**Errore. Il segnalibro non è definito.**. At 24 hours more than 50% of the radiopharmaceutical was cleared from these organs.

An high radioligand accumulation was observed in the tumors at 1 and 4 hours post injection (22.69±5.36 and 23.69±1.74 %ID/g respectively). When the receptors were blocked by a co-injection of an excess of the same cold peptide, the tumor uptake was found to be about 80% less compared to the 4-hour time point and this also holds for the other SSTR-positive organs.

At the 24 hours time point a good clearance was observed for all non-tumor and non-specific tissues, the only exception being the kidney, where the uptake remained high (6.69±0.70%ID/g).

111-Indium was the second radiometal used for DOTA-Peptide 1 radiolabeling. $^{111}$In is a γ-emitter with radiation energy of 0,171 and 0,245 MeV 90,94%, but it can used for therapeutic purpose, because 111-Indium is a Auger electron emitter (14.7 Auger yield, Auger energy 6.75 keV). Radioligand internalisation and retention assays and biodistribution studies were performed adopting the protocols described in previous session. This is a necessary step because different radiometals influence the pharmacological properties of radiopeptides.

*In vitro* assays were performed on rat pancreatic adenocarcinoma cell line (AR4-2J) stably expressing native SSTR2. Even in this case radioligand

internalisation assays were performed using $^{111}$In-DOTA-Tyr$^{3}$-octreotide/tate as references and it was demonstrated that internalisation is a time dependent process. Radioligand internalisation assay demonstrated a 6.59%±0.92 of internalised fraction after 4 hours of incubation. This dose is relatively higher in case of longer incubations (27.23%±1.6 of internalised radiopeptide at 24 hours time point).

The uptake results are appreciably lower if compared with the same experiment managed with $^{177}$Lu-DOTA Peptide 1. The motivations are mainly two: the first can be the radiometal changing that influences the peptide behaviour, the second regards the cell line adopted in this session. AR42J cells express wild type SSTR2 and receptor density is considerably lower if compared with the SSTR2 expression of transfected HEK-SSTR2.

Regarding cellular retention studies it can asserted that $^{111}$In-DOTA Peptide 1 maintained the same features presciently described, in fact cells retained 62.75%±3.04 of $^{111}$In-DOTA-Peptide1 after four hours of incubation.

*In vivo* biodistribution studies where performed on groups of healthy balb-c mice. Animals were injected with 10 pmol $^{111}$In-DOTA-Peptide 1 (0.15-0.2 MBq) and scarified 1, 4 and 24 hours post injection. To determine the non-specific uptake of radiolabelled peptide, a group of mice were injected with 20 nmol of DOTA-Peptide 1, 5 minutes before the injection of the radiopeptide. Results are expressed as % of injected dose/ grams of tissue. Pharmacokinetics studies demonstrated that the radiopeptide was rapidly cleared from circulation (0.95±7.8E-05 1 hour post injection, 0.67±0.0014 4 hours post injection, 0.18±0.0009 24 hours post injection). An high radioligand accumulation is observed in the pituitary gland at 1 (14.93±0.0088), 4 (7.45±0.0024) and 24 hours (8.10±0.0070) post injection, the stomach (1.13±0.0032 1 hour post injection, 1.04±0.0025 4 hours post injection, 0.46±0.0011 24 hours post injection) and the pancreas

(0.57±0.0022 1 hour post injection, 0.43±0.0021 4 hours post injection, 0.27±0.0001 24 hours post injection) too demonstrated a good uptake of the radiopharmaceutical. These are compatible with normal SSTRs expression with an exception of the kidneys that are responsible of the radiopharmaceutical clearance (13.39±0.001 1 hour post injection, 13.57±0.00572 4 hours post injection, 4.88±0.0009 24 hours post injection). The other organs demonstrated low uptake. At 24 hours time point a good clearance was observed for all tissues, the only exception are constituted by kidneys and pituitary gland, where the uptake remained high.

Affinity studies were also performed with a new technology: LigandTracer® produced by Ridgeview instruments AB. This instrument gives the possibility to perform different pharmacological assays on living cells in real time, as binding assays and uptake/ retention measurements.

The advantage of this instrumentation consists on the possibility to have a complete automate system and the possibility of using only a plate dish for all the study and consequently a small number of cells. Even if, this instrumentation seems to be very promising, it were noticed some problems that needs be solved to improve this methodology. The most important consists in the instrument software, that presents some difficulties in the data lecture.

Affinity studies were performed on NPA-87 cells expressing SSTR2 receptor with $^{111}$In-DOTA Peptide 1 and OctreoScan®, as control.

These are only preliminary results and the methodology requires important modifications. $IC_{50}$ and $B_{max}$ values are obtained (OctreoScan®: $IC_{50}$= 331.8 nM and $B_{max}$= 445.7; $^{111}$In-DOTA Peptide 1: $IC_{50}$=110.0 nM and $B_{max}$= 29.88). Moreover, by immunofluorescence studies, a precise different intracellular localization of SSTR2-ligand complex was observed at different times of the study, anyway, DTPA-Octreotide and DOTA-Peptide 1 have

generated similar answer, but it seems that DOTA-Peptide 1 have a higher potentiality to internalise.

Regarding pharmacological assays, immunofluorescence, a sensitive immunocytochemical method, was applied to examine SSTR2 internalization after DOTA-Peptide 1 treatment, peptide with an established interest for nuclear medicine.

Unlike radioactive isotopes, ligands to be tested for internalization will not experience alteration, which might affect the structure of the ligand and thus its biologic activity.

As conclusion, it can assert that high-affinity in SSTR2 binding is a prerequisite for an agonist to trigger SSTR2 internalization, and the behaviour of this compound seems reflect those of agonist.

Finally, it is important to emphasize that the second-generation compounds foreseen for *in vivo* SSTR2 targeting, such as octreotide, octreotate and the object of the study modified in position 3 and linked to DOTA, often have considerably better internalization capabilities than do the first-generation compound DTPA-octreotide[148].

The last session of the study regarded pro-apoptotic effects of SST-analogue. TUNEL assay was performed on AR42J cells treated with high concentration of DOTA-Peptide 1. Even if there are some studies in literature[149,150,151] that confirm the activation of the apoptotic pathway by the activation of SSTR2, no positivity were observed in TUNEL experiments.

Further considerations and investigations are required, especially the cytostatic effect due to SSTR2 activation have to be studied.

The cytotoxic signalling initiated by SST analogue is associated with the induction of wild type p53 and Bax[152] and in a study where an human adenocarcinoma breast cancer cell line (MCF-7) was used, it was demonstrated that no increase in p21, pRb or c-Myc was observed at 2 and

24 hr of Octreotide treatment and the lack of induction of p21 by octreotide is consistent with its ability to induce wild type p53 and apoptosis but not G1 arrest[152]. But this only a consideration, anyway it seems that SSTR2 modulates cell proliferation through SHP-1. Following recruitment to SSTR2 and subsequent activation, SHP-1 dephosphorylates various signaling molecules including growth factor receptors and nNOS, while enhancing the induction of $p27^{Kip1}$ and promoting cell cycle arrest[153].

Finally, it is important to underline that the α- or β-emitting SST analogues-tagged radionuclides shall elicit maximal cytotoxic response due not only to the triggering of apoptosis *via* induction of wt p53 and Bax by receptor-mediated signaling but also to the radiation induced damage following internalization. So it could predicted that treatment with SST analogs alone or in combination with radiation and/or chemotherapy could be most effective in treating wild type p53- and SSTR-expressing tumors.

# CONCLUSIONS

In recent years, knowledge in the SST field is considerately grown up, but a great number of dark points have still to be clarified and the developing of potent SST analogues for cancer treatment will require a more complete understanding of their intracellular actions and interactions.

Radiometal-labeled SST-analogues have demonstrated some or great benefit in the *in vivo* localization and PRRT of human tumors. The strategy that brought to an unquestionable positive result depends by a changing in strategy, in fact new chelators were adopted that allowed high thermodynamic and kinetic stability to the radiopeptides, while in terms of pharmacokinetic, pharmacodynamic and biological properties improvements are significant.

In this study, a new DOTA-based peptide (DOTA-Peptide 1) with diagnostic and therapeutic potential was characterized pharmacologically.

The limitation of this analogue is high the hydrophilicity of the molecule and a consequent kidney burning, determining a dose limiting organ in this type of targeted radiotherapy.

The peculiarity of the new analogue consists in the presence of two allil-glycines in the place of correspondent cysteines. Moreover, an aminoacidic substitutions is present in position 3, where a synthetic aminoacid is present.

The new SST analogue shows agonist characteristic with a great internalization in SSTR2-expressing cells and good biodistribution profile in mice bearing xenograft tumors.

Finally, it can conclude affirm that these results indicate that $^{111}In/^{177}Lu$-DOTA-Peptide 1 is a promising new SST-based radioligand for possible diagnosis and peptide radiocereptor therapy of tumors specifically expressing SSTR2.

**AKWNOLEDGEMENTS.**

This project was performed in collaboration with different universitary departments and research groups. For this reason I would like the to thank Laboratory of Peptides & Proteins, Chemistry & Biology (Department of chemistry Ugo Schiff, Florence) particularly Prof. Mauro Ginanneschi and Dr. Alessandra Di Cianni, that are the first responsibles of the accomplishment of this important project.

Secondarily, for binding assays for $IC_{50}$ determination, an acknowledgement have to be done to the Division of Cell Biology and Experimental Cancer Research (Institute of Pathology, University of Berne) directed by Prof. Jean Claude Reubi.

The first part of the study was performed in the Department of Radiology (Division of Radiological chemistry, Basel) direct by Prof. Helmut R. Maecke, during a short scientific mission supported by COST (COST BM0607 action).

It was an extremely exciting, absorbing and shaping experience, not only for the important results came out from the experiments, but also because it gave me the opportunity to enlarge my knowledge and to passionate me to this scientific field.

For this reason I would like to thank Dr. Melpomeni Fani and Dr. Maria Luisa Tamma for their precious scientific support, they were ideal teachers for me.

A particular acknowledgement have to be done to Prof . Helmut Maecke. He is a very charismatic gentleman and his passion to pharmacological research is contagious.

Finally, I would like to thank other all the Division of Radiological chemistry: Ksenia (for cells preparation too), Melpo, M. Luisa, Daniela, Rosalba, Luigi, Abiraj, Guillaume, Masen, Andreas and Jessica for the funny days spent in Basel.

The rest of the project was performed in Nuclear Medicine Department (University of Pisa) under the supervision of my supervisor Prof. Giuliano Mariani and my tutor Dr. Paola A. Erba. All my acknowledgements goes to them, they offered me an important opportunity for my learning after my master degree.

I would like to thank RIA lab (Maurizio, Massimo, Peppe, Tiziana and Valerio) where my invasions were always tolerate and Molecular Pathology lab, where my cells and me were friendly hosted!

Even if these years were hard and sometimes discouragement pervaded me, a lot of people helped and sustained me. First of all my family: my father and my mother always endowed me during these years. Thanks to them I could choose what I really like to do.

Moreover, I have to thank some friends and supporter: Luisa, Laura, Maria, Gabriella, Francesca, Sara, Pietro, Angela (my adventure and misadventure friend), my brother Alessandro and my sister Anna. The long conversations with them were always very inspiring.

Finally, an acknowledgement to Giovanni, with his deafening music, football, palatable dinners, his patience (not so much, if I am honest) and comprehension supported me during the compilation of this dissertation and during my PhD.

Thanks are due to the COST for financial support (COST BM0607 action).

# REFERENCES

[1] Brazeau P, Vale WW, Burgus R, Ling N, Butcher M, Rivier J, Guillemin R. Hypothalamic peptide that inhibits the secretion of immunoreactive pituitary growth hormone. Science 1973; 179: 77–79.

[2] Grimberg A. Somatostain and cancer: applying endocrinology to oncology Cancer. Biology & therapy Aug 2004; 3:8, 731-733.

[3] Epelbaum J, Dournaud P, Fodor M, Viollet C. The neurobiology of somatostatin. Crit Rev Neurobiol. 1994;8(1-2):25-44.

[4] Blum AM, Metwali A, Matthew RC, Cook G, Elliott D, Weinstock JV. Granuloma Tlymphocytes in murine schistosomiasis mansoni have somatostatin receptors and respond to somatostatin with decreased IFN-γ secretion. J Immunol 1992; 149: 3621–3626.

[5] Elliott DE, Blum AM, Li J, Metwaki A,Weinstock JV. Preprosomatostatin messenger RNAis expressed by inflammatory cells and induced by inflammatory mediators and cytokines. J Immunol 1998; 160: 3997–4003.

[6] Hayry P, Raisanen A, Ustinov J, Mennander A, Paavonen T. Somatostatin analog Lanreotide inhibits myocyte replication and several growth factors in allograft arteriosclerosis. FASEB J 1993; 7: 1055–1060.

[7] Patel YC. Somatostatin and its receptor family. Front Neuroendocrinol. 1999 Jul;20(3):157-98

[8] Patel YC, Greenwood M, Kent G, Panetta R, Srikant CB. Multiple gene transcripts of the somatostatin receptor SSTR2: tissue selective distribution and cAMP regulation. Biochem Biophys Res Commun. 1993 Apr 15;192(1):288-94.

[9] Csaba Z, Dournaud P. Cellular biology of somatostatin receptors. Neuropeptides. 2001 Feb;35(1):1-23.

[10] Casini Raggi C, Calabro A, Renzi D, Briganti V, Cianchi F, Messerini L, Valanzano R, Cameron Smith M, Cortesini C, Tonelli F, Serio M, Maggi M, Orlando C. Quantitative evaluation of somatostatin receptor subtype 2 expression in sporadic colorectal tumor and in the corresponding normal mucosa. Clin Cancer Res. 2002 Feb;8(2):419-27.

[11] Reubi JC, Laissue JA, Waser B, Steffen DL, Hipkin RW, Schonbrunn A. Immunohistochemical detection of somatostatin sst2a receptors in the lymphatic, smooth muscular, and peripheral nervous systems of the human gastrointestinal tract: facts and artifacts. J Clin Endocrinol Metab. 1999 84(8):2942-50.

[12] Kumar U, Sasi R, Suresh S, Patel A, Thangaraju M, Metrakos P, Patel SC, Patel YC. Subtype-selective expression of the five somatostatin receptors (hSSTR1-5) in human

pancreatic islet cells: a quantitative double-label immunohistochemical analysis. Diabetes. 1999 Jan;48(1):77-85.

[13] Reubi JC, Kappeler A, Waser B, Schonbrunn A, Laissue J. Immunohistochemical localization of somatostatin receptor sst2A in human pancreatic islets. J Clin Endocrinol Metab. 1998 Oct;83(10):3746-9.

[14] Portela-Gomes GM, Stridsberg M, Grimelius L, Oberg K, Janson ET. Expression of the five different somatostatin receptor subtypes in endocrine cells of the pancreas. Appl Immunohistochem Mol Morphol. 2000 Jun;8(2):126-32.

[15] Balster DA, O'Dorisio MS, Summers MA, Turman MA. Segmental expression of somatostatin receptor subtypes sst(1) and sst(2) in tubules and glomeruli of human kidney. Am J Physiol Renal Physiol. 2001 Mar;280(3):F457-65.

[16] Taniyama Y, Suzuki T, Mikami Y, Moriya T, Satomi S, Sasano H. Systemic distribution of somatostatin receptor subtypes in human: an immunohistochemical study. Endocr J. 2005 Oct;52(5):605-11.

[17] Reisine T, Bell GI. Molecular biology of somatostatin receptors. Endocr Rev 1995; 16: 427–442.

[18] Sedqi M, Roy S, Mohanraj D, Ramakrishnan S, Loh HH. Activation of rat thymocytes selectively upregulates the expression of somatostatin receptor subtype-1. Biochem Mol Biol Int. 1996 Feb;38(1):103-12.

[19] Patel YC. Molecular pharmacology of somatostatin receptor subtypes. J Endocrinol Invest 1997; 20: 348–367.

[20] Patel YC, Greenwood MT, Panetta R, Demchyshyn L, Niznik H, Srikant CB. The somatostatin receptor family. Life Sci 1995; 57: 1249–1265.

[21] Patel YC, Murthy KK, Escher E, Banville D, Spiess J, Srikant CB. Mechanism of action of somatostatin:An overview of receptor function and studies of themolecular characterization and purification of somatostatin receptor proteins. Metabolism 1990; 39(Suppl. 2): 63–69.

[22] Reubi JC, Maecke HR, Peptide-Based Probes for Cancer Imaging, The J of Nucl med Vol. 49 No. 11 November 2008.

[23] De Jong M, Valkema R, Jamar F,. Kvols LK,. Kwekkeboom DJ, Breeman WAP,. Bakker WH, Smith C, Pauwels S, Krenning EP Somatostatin Receptor-Targeted Radionuclide Therapy of Tumors: Preclinical and Clinical Findings Seminars in Nuclear Medicine, Vol 32, n° 2 (April), 2002: pp 133-140.

[24] Reubi JC, Schaer JC, Waser B, Mengod G Expression and localization of somatostatin receptor SSTR1, SSTR2, and SSTR3 messenger RNAs in primary human tumors using *in situ* hybridization. Cancer Res 1994 54:3455–3459.

[25] Reubi JC, Waser B, Schaer JC, Markwalder R Somatostatin receptors in human prostate and prostate cancer. 1995 J Clin Endocrinol Metab 80:2806–2814.

[26] Panetta R, Patel YC Expression of mRNA for all five human somatostatin receptors (hSSTR1–5) in pituitary tumors. 1995 Life Sci 56:333–342.

[27] Schulz S, Schmitt J, Wiborny D, Schmidt H, Olbricht S, Weise W, Roessner A, Gramsch C, Hollt V Immunocytochemical detection of somatostatin receptors sst1, sst2A, sst2B, and sst3 in paraffin-embedded breast cancer tissue using subtype-specific antibodies. 1998 Clin Cancer Res 4:2047–2052.

[28] Hofland LJ, Lamberts SW.The pathophysiological consequences of somatostatin receptor internalization and resistance. Endocr Rev. 2003 Feb;24(1):28-47.

[29] Krenning EP, Bakker WH, Breeman WAP, Koper JW, Kooij PPM, Ausema L, Lameris JS, Reubi JC, Lamberts SWJ. Localisation of endocrine-related tumours with radioiodinated analogue of somatostatin. Lancet 1989; I:242–244.

[30] Lopci E, Nanni C, Rampin L, Rubello D, Fanti S. Clinical applications of 68Ga-DOTANOC in neuroendocrine tumours. Minerva Endocrinol. 2008 Sep;33(3):277-81.

[31] Arnold C. Neuroendocrine tumors of the gastrointestinal tract]Praxis (Bern 1994). 2007 Jan 10;96(1-2):19-28.

[32] Taboada GF, Luque RM, Bastos W, Guimaraes RF, Marcondes JB, Chimelli LM, Fontes R, Mata PJ, Filho PN, Carvalho DP, Kineman RD, Gadelha MR. Quantitative analysis of somatostatin receptor subtype (SSTR1-5) gene expression levels in somatotropinomas and non-functioning pituitary adenomas. Eur J Endocrinol. 2007 Jan;156(1):65-74.

[33] Vikic-Topic S, Raisch KP, Kvols LK, Vuk-Pavlovic S. Expression of somatostatin receptor subtypes in breast carcino ma, carcinoid tumor, and renal cell carcinoma. J Clin Endocrinol Metab. 1995 Oct;80(10):2974-9.

[34] Kimura N, Pilichowska M, Date F, Kimura I, Schindler M. Immunohistochemical expression of somatostatin type 2A receptor in neuroendocrine tumors. Clin Cancer Res. 1999 Nov;5(11):3483-7.

[35] Arena S, Barbieri F, Thellung S, Pirani P, Corsaro A, Villa V, Dadati P, Dorcaratto A, Lapertosa G, Ravetti JL, Spaziante R, Schettini G, Florio T. Expression of somatostatin receptor mRNA in human meningiomas and their implication in in vitro antiproliferative activity.J Neurooncol. 2004 Jan;66(1-2):155-66.

[36] Feindt J, Becker I, Blomer U, Hugo HH, Mehdorn HM, Krisch B, Mentlein R. Expression of somatostatin receptor subtypes in cultured astrocytes and gliomas. J Neurochem. 1995 Nov;65(5):1997-2005.

[37] Rostomily RC, Elias M, Deng M, Elias P, Born DE, Muballe D, Silbergeld DL, Futran N, Weymuller EA, Mankoff DA, Eary J. Clinical utility of somatostatin receptor scintigraphic imaging (octreoscan) in esthesioneuroblastoma: a case study and survey of somatostatin receptor subtype expression. Head Neck. 2006 Apr;28(4):305-12.

[38] Unger N, Serdiuk I, Sheu SY, Walz MK, Schulz S, Schmid KW, Mann K, Petersenn S. Immunohistochemical determination of somatostatin receptor subtypes 1, 2A, 3, 4, and 5 in various adrenal tumors. Endocr Res. 2004 Nov;30(4):931-4.

[39] Kolby L, Wangberg B, Ahlman H, Tisell LE, Fjalling M, Forssell-Aronsson E, Nilsson O. Somatostatin receptor subtypes, octreotide scintigraphy, and clinical response to octreotide treatment in patients with neuroendocrine tumors. World J Surg. 1998 Jul;22(7):679-83.

[40] Fujita T, Yamaji Y, Sato M, Murao K, Takahara J. Gene expression of somatostatin receptor subtypes, SSTR1 and SSTR2, in human lung cancer cell lines. Life Sci. 1994;55(23):1797-806.

[41] Oberg KE, Reubi JC, Kwekkeboom DJ, Krenning EP. Role of somatostatins in gastroenteropancreatic neuroendocrine tumor development and therapy. Gastroenterology. 2010 Sep;139(3):742-53, 753.e1.

[42] Kulaksiz H, Eissele R, Rössler D, Schulz S, Höllt V, Cetin Y, Arnold R. Identification of somatostatin receptor subtypes 1, 2A, 3, and 5 in neuroendocrine tumours with subtype specific antibodies. Gut. 2002 Jan;50(1):52-60.

[43] Wermer P: Genetic aspects of adenomatosis of endocrine glands. Am J Med 1954, 16:363.

[44] Brandi ML, Gagel RF, Angeli A, Bilezikian JP, Beck-Peccoz P, Bordi C, Conte-Devolx B, Falchetti A, Gheri RG, Libroia A, Lips CJ, Lombardi G, Mannelli M, Pacini F, Ponder BA, Raue F, Skogseid B, Tamburrano G, Thakker RV, Thompson NW, Tomassetti P, Tonelli F, Wells SA Jr, Marx SJ: Guidelines for diagnosis and therapy of MEN type 1 and type 2. J Clin Endocrinol Metab 2001, 86:5658-71.

[45] Anlauf M, Perren A, Meyer CL, Schmid S, Saremaslani P, Kruse ML, Weihe E, Komminoth P, Heitz PU, Klöppel G: Precursor lesions in patients with multiple endocrine neoplasia type 1-associated duodenal gastrinomas. Gastroenterology 2005, 128:1187-98.

[46] Emmert-Buck MR, Lubensky IA, Dong Q, Manickam P, Guru SC, Kester MB, Olufemi SE, Agarwal S, Burns AL, Spiegel AM, Collins FS, Marx SJ, Zhuang Z, Liotta LA, Chandrasekharappa SC, Debelenko LV: Localization of the multiple endocrine neoplasia type I (MEN1) gene based on tumor loss of heterozygosity analysis. Cancer Res 1997, 57:1855-8.

[47] Friedman E, Sakaguchi K, Bale AE, Falchetti A, Streeten E, Zimering M, Weinstein L, Mc Bride WO, Nakamura Y, Brandi ML, Norton JA, Aurbach GD, Spiegel AM, Marx SJ: Clonality of parathyroid tumors in familial multiple endocrine neoplasia type 1. N Engl J Med 1989, 321:213-8.

[48] Bartsch DK, Langer P, Rothmund M. Surgical aspects of gastrinoma in multiple endocrine neoplasia type 1. Wien Klin Wochenschr 2007; 119: 602-8.

[49] Zhou H, Schweikert HU, Wolff M, Fischer HP. Primary peripancreatic lymph node gastrinoma in a woman with MEN1. J Hepatobiliary Pancreat Surg 2006; 13: 477-81.

[50] Díaz R, Aparicio J, Pous S, Dolz JF, Calderero V. Primary hepatic gastrinoma. Dig Dis Sci 2003; 48: 1665-7.

[51] Raue F, Frank-Raue K, 2007 Multiple Endocrine Neoplasia Type 2: 2007 Update. Horm Res 68:101-104.

[52] Kouvaraki MA, Shapiro SE, Perrier ND, et al, 2005 RET proto-oncogene: a review and update of genotype-phenotype correlations in hereditary medullary thyroid cancer and associated endocrine tumors. Thyroid 15: 531-544.

[53] Vikic-Topic S, Raisch KP, Kvols LK, Vuk-Pavlovic S; Expression of somatostatin receptor subtypes in breast carcinoma, carcinoid tumor and renal cell carcinoma. J Clin Endocrinol Metab 1995 oct;80(10):2974-9.

[54] Hansson J, Bjartell A, Gadaleanu V, Dizeyi N, Abrahamsson PA. Expression of somatostatin receptor subtypes 2 and 4 in human benign prostatic hyperplasia and prostatic cancer. Prostate. 2002 Dec 1;53(4):330.

[55] De Jong M, Bernard BF, De Bruin E, Van Gameren A, Bakker WH, Visser TJ, Mäcke HR, Krenning EP. Internalization of radiolabelled [DTPA$^{0}$]octreotide and [DOTA$^{0}$,Tyr$^{3}$]octreotide: peptides for somatostatin receptor-targeted scintigraphy and radionuclide therapy. Nucl Med Commun. 1998 Mar;19(3):283-8.

[56] Bushnell DL, Menda Y, Madsen MT, Link BK, Kahn D, Truhlar SM, Juweid M, Shannon M, Murguia JS. 99mTc-depreotide tumour uptake in patients with non-Hodgkin's lymphoma. Nucl Med Commun. 2004 Aug;25(8):839-43.

[57] Schlumberger MJ Papillary and follicular thyroid carcinoma. N Engl J Med 1998 338:297–306.

[58] M. Druckenthaner, C. Schwarzer, C. Ensinger, M. Gabriel, R. Prommegger, G. Riccabona, C. Decristoforo , Evidence for Somatostatin receptor 2 in thyroid tissue Regulatory Peptides 138 (2007) 32–39.

[59] Hemminki K, Li X. Incidence trends and risk factors of carcinoid tumors. A nationwide epidemiologic study from Sweden. Cancer 2001; 92:2204-2210.

[60] Berge T, Linnel F. Carcinoid tumor. Frequency in a defined population during a 12-year-period. Acta Pathol Microbiol Scand 1976; 84:322-330.

[61] Appetecchia M, Baldelli R. Somatostatin analogues in the treatment of gastroenteropancreatic neuroendocrine tumours, current aspects and new perspectives. J Exp Clin Cancer Res. 2010 Mar 2;29:19.

[62] Modlin IM, Lye KD, Kidd M. A 5-decade analysis of 13,715 carcinoid tumors. Cancer 2003; 79:943-957.

[63] Maggard MA, O'Connel JB, Ko CY. Update population based review of carcinoid tumors. Ann Surg 2004; 240:117-122.

[64] McGory ML, Maggard MA, O'Connel JB, Kang H, Ko CY. Malignancy of appendix: beyond case series reports. Dis Colon Rectum 2005; 48:2264-2271.

[65] Capella C, Solcia E, Sobin LH, Arnold A. Endocrine tumors of the esophagus. In Hamilton SR, Aatonen LA (eds); Pathology and genetics. Tumors of the digestive system. WHO classification of tumors. IARC, Lyon, 2000; pp 26-27.

[66] Kloppel G, Rindi G, Anlauf M, Perren A, Komminoth P. Site specific biology and pathology of gastroenteropancreatic neuroendocrine tumors. Wirchovs Arch 2007; 451(1):9-27.

[67] Rosato L. I tumori neuroendocrini. Manuale di trattamento diagnostico e terapeutico. Seconda edizione 2007 GS editrice.

[68] Nakayama Y, Wada R, Yajima N, Hakamada K, Yagihashi S. Profiling of somatostatin receptor subtype expression by quantitative PCR and correlation with clinicopathological features in pancreatic endocrine tumors. Pancreas. 2010 Nov;39(8):1147-54.

[69] Janson ET, Oberg K Neuroendocrine tumors--somatostatin receptor expression and somatostatin analog treatment. Cancer Chemother Biol Response Modif. 2003;21:535-46.

[70] Mato E, Matías-Guiu X, Chico A, Webb SM, Cabezas R, Berná L, De Leiva A. Somatostatin and somatostatin receptor subtype gene expression in medullary thyroid carcinoma. J Clin Endocrinol Metab. 1998 Jul;83(7):2417-20.

[71] Cramer JD, Fu P, Harth KC, Margevicius S, Wilhelm SM. Analysis of the rising incidence of thyroid cancer using the Surveillance, Epidemiology and End Results national cancer data registry. Surgery. 2010 Dec;148(6):1147-52.

[72] Pisarek H, Stepień T, Kubiak R, Borkowska E, Pawlikowski M. Expression of somatostatin receptor subtypes in human thyroid tumors: the immunohistochemical and molecular biology (RT-PCR) investigation. Thyroid Res. 2009 Jan 27;2(1):1.

[73] Righi L, Volante M, Tavaglione V, Billè A, Daniele L, Angusti T, Inzani F, Pelosi G, Rindi G, Papotti M. Somatostatin receptor tissue distribution in lung neuroendocrine tumours: a clinicopathologic and immunohistochemical study of 218 'clinically aggressive' cases. Ann Oncol. 2010 Mar;21(3):548-55.

[74] Watt HL, Kharmate G, Kumar U. Biology of somatostatin in breast cancer Molecular and Cellular Endocrinology 286 (2008) 251–261.

[75] Vogelstein B, Kinzler K, Has the breast cancer gene been found? Cell 1994; 9, 1–3.

[76] Harris J, Lippman M, Veronesi U, Willet W, Breast cancer. N. Engl. J. Med. 1993; 327, 319–328, 390–398, 473–480.

[77] Kumar U, Grigorakis SI, Watt HL, Sasi R, Snell L, Watson P, Chaudhari S. Somatostatin receptors in primary human breast cancer: quantitative analysis of mRNA for subtypes 1-5 and correlation with receptor protein expression and tumor pathology. Breast Cancer Res Treat. 2005 Jul;92(2):175-86.

[78] Chow WH, Devesa SS, Warren JL. The rising incidence of renal carcinoma in the United States of America. JAMA 1999; 282: 1629-312.

[79] Shvarts O, Lepper JT, Figlin RA, Belldegrun AS Renal cell carcinoma 2005, New frontiers in staging, prognostication and targeted therapy. J urol. 2005; 173: 1853-62.

[80] Russo P, O' Brien MF, Surgical intervention in patients with metastatic renal cell carcinoma: Metastasectomy and cytoreductive nephrectomy. Urol clin North am 2008; 35: 679-86.

[81] Hoffman NE, Gillet MD, Cheville JC, Difference in organ system of distant matastases by mRCC subtypes J urol 2008;180: 474-7.

[82] Bushnell DL, Menda Y, Madsen MT, Link BK, Kahn D, Truhlar SM, Juweid M, Shannon M, Murguia JS. 99mTc-depreotide tumour uptake in patients with non-Hodgkin's lymphoma. Nucl Med Commun. 2004 Aug;25(8):839-43.

[83] Raderer M, Traub T, Formanek M, Virgolini I, Osterreicher C, Fiebiger W, Penz M, Jäger U, Pont J, Chott A, Kurtaran A. Somatostatin-receptor scintigraphy for staging and follow-up of patients with extraintestinal marginal zone B-cell lymphoma of the mucosa associated lymphoid tissue (MALT)-type. Br J Cancer. 2001 Nov 16;85(10):1462-6.

[84] Guillemin R, Gerich JE, Somatostatin: physiological and clinical significance, Annu Rev Med 1976 27:379-388.

[85] Reisine T, Bell GI, Molecular biology of somagostatin receptors. Endocr Rev, 1995 16:427-442.

[86] Patel, YC, Srikant, CB. Subtype selectivity of peptide analogs for all five cloned human somatostatin receptors (hSSTR 1-5). Endocrinology, 1994 135: 2814-2817.

[87] Grimberg A, Mechanism by which IGF-I may promote cancer. Cancer Biol Ther 2003;2:630-5.

[88] Lamberts SW, de Herder WW, Hofland LJ, Somatostatin analogs in the diagnosis and treatment of cancer. Trends Endocrinol Metab 2002;13:451-7.

[89] Barrie R, Woltering EA, Hajarizadeh H, Mueller C, Ure T & Fletcher WS 1993 Inhibition of angiogenesis by somatostatin and somatostatin-like compounds is structurally dependent. Journal of Surgical Research 55 446–450.

[90] Patel PC, Barrie R, Hill N, Landeck S, Kurozawa D & Woltering EA 1994 Postreceptor signal transduction mechanisms involved in octreotide-induced inhibition of angiogenesis. Surgery 116 1148–1152.

[91] Watson JC, Balster DA, Gebhardt BM, O'Dorisio TM, O'Dorisio MS, Espenan GD, Drouant GJ & Woltering EA 2001 Growing vascular endothelial cells express somatostatin subtype 2 receptors. British Journal of Cancer 85 266–272.

[92] Florio T. Molecular mechanism of antiproliferative activity of somatostatin receptors (SSTRs) in nuroendocrine tumors; Frontiers in bioscience 13, 822-840, Jan 1, 2008.

[93] Reubi JC, Laissue JA: Multiple actions of somatostatin in neoplastic disease. Trends Pharmacol Sci 1995, 16, 110-115.

[94] Weckbecker G, LewisI , Albert R, Schmid HA, Hoyer D Bruns C: Opportunities in somatostatin research: biological, chemical and therapeutic aspects. Nat Rev Drug Discov, 2(12), 999-1017 (2003).

[95] Sharma K, Patel YC, Srikant CB, Induction of wild type p53, Bax and acidic endonuclease during somatostatin-signaled apoptosis in MCF-7 human breast cancer cells. Int J cancer 1988,76:259-66.

[96] Pagliacci MC, Tognellini R, Grignani F, Nicoletti I, Inhibition of human breast cancer cell (MCF-7) growth in vitro by the somatostatin analog SMS 201–995: effects on cell cycle parameters and apoptotic cell death. Endocrinology 1991 129 2555–2562.

[97] Rochaix P, Delesque N, Esteve JP, Saint-Laurent N, Voight JJ, Vaysse N, Susini C & Buscail L 1999 Gene therapy for pancreatic carcinoma: local and distant antitumor effects after somatostatin receptor sst2 gene transfer. Human Gene Therapy 10 995–1008.

[98] Grozinsky-Glasberg S, Shimon I, Korbonits1 M, Grossman AB, Somatostatin analogues in the control of neuroendocrine tumours: efficacy and mechanisms Endocrine-Related Cancer (2008) 15 701–720.

[99] Friess H, Buchler M, Beglinger C. Weber A, Kunz J, Fritsch K, Dennler HJ, Beger HG. Low-dose octreotide treatment is not effective in patients with advanced pancreatic cancer. Pancreas 1993; 8: 540–545.

[100] Schally AV, Szepeshazi K, Nagy A et al. New approaches to therapy of cancers of the stomach, colon and pancreas based on peptide analogs. Cell Mol Life Sci 2004; 61: 1042–1068.

[101] Lamberts SW, van Koetsveld P, Hofland LJ. The interrelationship between the anti-mitotic action of the somatostatin analog octreotide and that of cytostatic drugs and suramin. Int J Cancer 1991; 48: 938–941.

[102] Krenning, E, Bakker, WH, Breeman, WA, et al. Localisation of endocrine-related tumours with radioiodinated analogue of somatostatin. Lancet, 1989 1: 242-244.

[103] Wester, H, Brockmann, J, Rosch, F, et al. PET-pharmacokinetics of 18F-octreotide: a comparison with $^{67}$Ga-DFO- and $^{86}$Y-DTPA-octreotide. Nucl Med Biol, 1997 24(4): 275-286.

[104] Froidevaux, S, Eberle, AN, Christe, M, et al. Neuroendocrine tumor targeting: study of novel gallium labeled somatostatin radiopeptides in a rat pancreatic tumor model. Int J Cancer, 2002 98(6): 930-937.

[105] Henze M, Schuhmacher J, Hipp P, Kowalski J, Becker DW, Doll J, Macke HR, Hofman M, Debus J, Haberkorn U, PET imaging of somatostatin receptors using [$^{68}$Ga]DOTA-D-Phe$^{1}$-Tyr$^{3}$-octreotide: first results in patients with meningiomas. J Nucl Med, 2001 42(7): 1053-1056.

[106] Otte, A, Mueller-Brand, J, Dellas, S, Nitzsche, E, Herrmann, R, Maecke, H. Yttrium-90-labelled somatostatin-analogue for cancer treatment. Lancet, **1998**: 417-418.

[107] Bodei L, Cremonesi M, Grana C, Rocca P, Bartolomei M, Chinol M, Paganelli G, Receptor radionuclide therapy with 90Y-[DOTA]$^{0}$-Tyr$^{3}$-octreotide ($^{90}$Y-DOTATOC) in neuroendocrine tumours. Eur J Nucl Med Mol Imaging, 2004 31(7): 038-46.

[108] Reubi, JC. Peptide receptors as molecular targets for cancer diagnosis and therapy. Endocr Rev, 24(4): 389-427.

[109] Reubi, JC, Schaer, JC, Waser, B, Wenger, S.; Heppeler, A.; Schmitt, J. S.; Macke, H. R. Affinity Profiles for Human Somatostatin Receptor Subtypes SST1-SST5 of Somatostatin Radiotracers Selected for Scintigraphic and Radiotherapeutic Use. Eur. J. Nucl. Med. 2000, *27*,273–282.

[110] De Jong M, Breeman WAP, Valkema R, Bernard BF, Krenning EP, Combination Radionuclide Therapy Using 177Luand 90Y-Labeled Somatostatin Analogs, J of nucl med Jan 2005Vol. 46, No. 1.

[111] Rolleman EJ, Melis M, Valkema R, Boerman OC, Krenning EP, de Jong M. Kidney protection during peptide receptor radionuclide therapy with somatostatin analogues. Eur J Nucl Med Mol Imaging. 2010 May;37(5):1018-31.

[112] Melis M, Bijster M, de Visser M, Konijnenberg MW, de Swart J, Rolleman EJ, Boerman OC, Krenning EP, De Jong M, Dose-response effect of Gelofusine on renal uptake and retention of radiolabelled octreotate in rats with CA20948 tumours Eur J Nucl Med Mol Imaging (2009) 36:1968–1976.

[113] Michel RB, Rosario AV, Andrews PM, Goldenberg DM, Mattes MJ. Therapy of small subcutaneous B-lymphoma xenografts with antibodies conjugated to radionuclides emitting low-energy electrons. Clin Cancer Res. 2005 Jan 15;11:777-86.

[114] Koenig JA, Edwardson JM, Endocytosis and recycling of G-protein-coupled receptors. Trends Pharmacol Sci (1997) Aug 18(8):276–287.

[115] Ginj M, Zhang H, Waser B, Cescato R, Wild D, Wang X, Erchegyi J, Rivier J, Mäcke HR, Reubi JC, Radiolabeled somatostatin receptor antagonists are preferable to agonists for in vivo peptide receptor targeting of tumors. Proc Natl Acad Sci U S A. 2006 Oct 31;103(44):16436-41. Epub 2006 Oct 2.

[116] O'Donoghue, JA, Wheldon, TE, Targeted radiotherapy using Auger electron emitters. Phys Med Biol, 1996 41: 1973-1992.

[117] Ferguson, SSG. Evolving concepts in G protein-coupled receptor endocytosis: the role in receptor desensitization and signaling. Pharmacol Rev, 2001 53: 1-24.

[118] Prossnitz, ER. Novel roles for arrestins in the post-endocytic trafficking of G-protein coupled receptors. Life Sci, 2004 75: 893-899.

[119] Hipkin, R, Friedman, J, Clark, RB, Eppler, CM, Schonbrunn, A. Agonist-induced desensitization, internalization and phosphorylation of the sst2A somatostatin receptor. J Biol Chem, 1997 272(21): 13869-13876.

[120] Schwartkop, C, Kreienkamp, HJ, Richter, D. Agonist-independent internalization and activity of a Cterminally truncated somatostatin receptor subtype 2 (D349). J Neurochem, 1999 72: 1275-1282.

[121] Roth, A, Kreienkamp, HJ, Meyerhof, W, Richter, D. Phosphorylation of four amino acid residues in the carboxyl terminus of the rat somatostatin receptor subtype 3 is crucial for its desensitization and internalization. J Biol Chem, 1997 272: 23769-23774.

[122] Elberg, G, Hipjin, RW, Schonbrunn, A. Homologous and heterologous regulation of somatostatin receptor 2. Mol Endocrinol, 2002 16(11): 2502-2514.

[123] Liu, Q, Reubi, JC, Wang, Y, Knoll, BJ, Schonbrunn, A. In vivo phosphorylation of the somatostatin 2A receptor in human tumors. J Clin Endocrinol Metab, 2003 88(12): 6073-6079.

[124] Grubbs, R. H. Olefin Metathesis. Tetrahedron 2004, 60, 71187-7140.

[125] Blackwell, H. E.; Sadowsky, J. D.; Howard, R. J.; Sampson, J. N.; Chao, J. A.; Steinmetz, W. E.; O'Leary, D. J.; Grubbs, R. H. Ring-Closing Metathesis of Olefinic Peptides: Design Synthesis, and Structural Characterization of Macrocyclic Helical Peptides. J. Org. Chem. 2001, 66, 5291-5302.

[126] Stymiest, J. L.; Mitchell, B. F; Wong, S.; Vederas, J. C. Synthesis of Oxytocyn Analogues with Replacement of Sulfur by Carbon Gives Potent Antagonists with Increased Stability. J. Org. Chem. 2005, 70, 7799–7809.

[127] Reichwein, J. F.; Versluis, C.; Liskamp, R. B. Synthesis of Cyclic Peptides by Ring Closing Metathesis. J. Org. Chem. 2000, 65, 6187-6195.

[128] Carotenuto, A.; D'Addona, D.; Rivalta, E.; Chelli, M.; Papini, A. M.; Rovero, P.; Ginanneschi, M. Synthesis of a Dicarba-Analogue of Octreotide Keeping the Type II' $\beta$-Turn of the Pharmacophore in Water Solution. Lett. Org. Chem. 2005, *2*, 274-279.

[129] D'Addona D, Carotenuto A., Novellino E., Piccand V., Reubi J.C., Alessandra Di Cianni, Francesca Gori, Anna Maria Papini and Mauro Ginanneschi. 'Novel $sst_5$-selective Somatostatin Dicarba-analogues. Synthesis and Conformational-affinity Relationship' J Med Chem 2008, 51, 512-520.

[130] Tulipano G, Stumm R, Pfeiffer M, Kreienkamp HJ, Volker Höllt, Schulz S, Differential β-Arrestin Trafficking and Endosomal Sorting of Somatostatin Receptor Subtypes THE J OF BIOL CHEM Vol. 279, No. 20, Issue of May 14, pp. 21374–21382, 2004.

[131] Lamberts, S. W.; Van der Lely, A. J.; Hofland, L. J. New Somatostatin Analogs: Will They Fulfill Old Promises? *Eur. J. Endocrinol.* **2002**, *146*, 701–705.

[132] Behe M, Behr TM, Schmalor W, Herbst B, Gotthardt M. Indium-111 labelled GLP-1 for in vivo diagnostic of insulinomas. J Nucl Med. 2002; 43(suppl):92P.

[133] Nock B, Nikolopoulou A, Chiotellis E, [$^{99m}$Tc]demobesin 1, a novel potent bombesin analogue for GRP receptor-targeted tumour imaging. Eur J Nucl Med. 2003;30:247–258.

[134] Langer M, La Bella R, Garcia-Garayoa E, Beck-Sickinger AG. 99mTc-labeled neuropeptide Y analogues as potential tumor imaging agents. Bioconjug Chem. 2001;12:1028 –1034.

[135] Liu Z, Shi J, Jia B, Yu Z, Liu Y, Zhao H, Li F, Tian J, Chen X, Liu S, Wang F. $^{90}$Y-Labeled Two Multimeric RGD Peptides RGD4 and 3PRGD2 for Integrin Targeted Radionuclide Therapy. Mol Pharm. 2011 Jan 19.

[136] Warner RRR, O'Dorisio TM, Radiolabeled Peptides in Diagnosis and Tumor Imaging: Clinical Overview Seminars in Nuclear Medicine, Vol 32, No 2 (April), 2002: pp 79-83.

[137] Paganelli G, Bodei L, Handkiewicz Junak D, Rocca P, Papi S, Lopera Sierra M, Gatti M, Chinol M, Bartolomei M, FiorenzaMet al. 2002 $^{90}$Y-DOTA-D-Phe$^1$-Tyr$^3$-octreotide in therapy of neuroendocrine malignancies. Biopolymers 66 393–398.

[138] Valkema R, Pauwels S, Kvols LK, Barone R, Jamar F, Bakker WH, Kwekkeboom DJ, Bouterfa H, Krenning D J Kwekkeboom SRI and PRRT in GEPNETs EP 2006 Survival and response after peptide receptor radionuclide therapy with [$^{90}$Y-DOTA$^0$,Tyr$^3$]octreotide in patients with advanced gastroenteropancreatic neuroendocrine tumors. Seminars in Nuclear Medicine 36 147–156.

[139] Erion JL, Bugaj JE, Schmidt MA, Wilhelm RR & Srinivasan A 1999 High radiotherapeutic efficacy of [Lu-177]- DOTA-Y$^3$-octreotate in a rat tumor model. J of Nucl Med 40 (Suppl) 223.

[140] Kwekkeboom DJ, Bakker WH, Kam BL, Teunissen JJ, Kooij PP, de Herder WW, Feelders RA, van Eijck CH, de Jong M, Srinivasan A, Erion JL, Krenning EP (2003) Treatment of patients with gastro-entero-pancreatic (GEP) tumours with the novel radiolabelled somatostatin analogue [$^{177}$Lu-DOTA$^{0}$-Tyr$^{3}$]octreotate. Eur J Nucl Med Mol Imaging 30: 417–422.

[141] Esser JP, Krenning EP, Teunissen JJ, Kooij PP, van Gameren AL, Bakker WH Kwekkeboom DJ, Comparison of [$^{177}$Lu-DOTA$^{0}$-Tyr$^{3}$]octreotate and [$^{177}$Lu-DOTA$^{0}$-Tyr$^{3}$]octreotide: which peptide is preferable for PRRT? European Journal of Nuclear Medicine and Molecular Imaging 2006-33 1346–1351.

[142] Ginj M, Chen J, Walter MA, Eltschinger V, Reubi JC, Maecke HR. Preclinical evaluation of new and highly potent analogues of octreotide for predictive imaging and targeted radiotherapy. Clin Cancer Res. 2005 Feb 1;11(3):1136-45.

[143] Prasad V, Baum RP. Biodistribution of the Ga-68 labeled somatostatin analogue DOTA-NOC in patients with neuroendocrine tumors: characterization of uptake in normal organs and tumor lesions. Q J Nucl Med Mol Imaging. 2010 Feb;54(1):61-7.

[144] Scarpignato C, Pelosini I, Somatostatin analogs for cancer treatment and diagnosis.an overview; Chemother 2001; 47:1-29.

[145] Gibril F, Gensen RT, Diagnostic uses of radiolabelled somatostatin receptor analogues in gastroenteropancreatic endocrine tumors. Digest Liver Dis 2004,36 Suppl 1:106-120.

[146] Gabriel M, Decristoforo C, Kendler D, Dobrozemsky G, Heute D, Uprimny C, Kovacs P, Von Guggenberg E, Bale R, Virgolini IJ. 68Ga-DOTA-Tyr3-octreotide PET in neuroendocrine tumors: comparison with somatostatin receptor scintigraphy and CT. J Nucl Med. 2007 Apr;48(4):508-18.

[147] Middendorp M, Selkinski I, Happel C, Kranert WT, Grünwald F. Comparison of positron emission tomography with [(18)F]FDG and [(68)Ga]DOTATOC in recurrent differentiated thyroid cancer: preliminary data. Q J Nucl Med Mol Imaging. 2010 Feb;54(1):76-83.

[148] Cescato R, Schulz S, Waser B, Eltschinger V, Rivier JE, Wester HJ, Culler M, Ginj M, Liu Q, Schonbrunn A, Reubi JC. Internalization of sst2, sst3, and sst5 receptors: effects of somatostatin agonists and antagonists. J Nucl Med. 2006 Mar;47(3):502-11.

[149] He Y, Yuan XM, Lei P, Wu S, Xing W, Lan XL, Zhu HF, Huang T, Wang GB, An R, Zhang YX, Shen GX The antiproliferative effects of somatostatin receptor subtype 2 in breast cancer cells. Acta Pharmacol Sin. 2009 Jul;30(7):1053-9.

[150] Ferrante E, Pellegrini C, Bondioni S, Peverelli E, Locatelli M, Gelmini P, Luciani P, Peri A, Mantovani G, Bosari S, Beck-Peccoz P, Spada A, Lania A. Octreotide promotes apoptosis in human somatotroph tumor cells by activating somatostatin receptor type 2. Endocr Relat Cancer. 2006 Sep;13(3):955-62.

[151] Vernejoul F, Faure P, Benali N, Calise D, Tiraby G, Pradayrol L, Susini C, Buscail L. Antitumor effect of in vivo somatostatin receptor subtype 2 gene transfer in primary and metastatic pancreatic cancer models. Cancer Res. 2002 Nov 1;62(21):6124-31.

[152] K Sharma CB Srikant Induction of wild type p53, bax, and acidic endonuclease duringsomatostatin-signaled apoptosis in MCF-7 human breast cancer cells Int. J. Cancer: 76, 259–266 (1998) 1998Wiley-Liss, Inc.

[153] Ferjoux, G., Lopez, F., Esteve, J.-P., Ferrand, A., Vivier, E., Vely, F., Saint- Laurent, N., Pradayrol, L., Buscail, L., Susini, C., Critical role of Src and SHP-2 in sst2 somatostatin receptor-mediated activation of SHP-1 and inhibition of cell proliferation. Mol. Biol. Cell 2003 14, 3911–3928.